

2010

Targets of Hsa-miR-488* in Human Prostate Carcinoma Cells

Jinani E. Slaibi
Cleveland State University

Follow this and additional works at: <https://engagedscholarship.csuohio.edu/etdarchive>

 Part of the [Biology Commons](#)

How does access to this work benefit you? Let us know!

Recommended Citation

Slaibi, Jinani E., "Targets of Hsa-miR-488* in Human Prostate Carcinoma Cells" (2010). *ETD Archive*. 677.
<https://engagedscholarship.csuohio.edu/etdarchive/677>

This Thesis is brought to you for free and open access by EngagedScholarship@CSU. It has been accepted for inclusion in ETD Archive by an authorized administrator of EngagedScholarship@CSU. For more information, please contact library.es@csuohio.edu.

TARGETS OF HSA-MIR-488* IN HUMAN PROSTATE CARCINOMA CELLS

JINANI E. SLAIBI

Bachelor of Science in Biology

Cleveland State University

May, 2008

Submitted in partial fulfillment of requirements for the degree

MASTER OF SCIENCE IN BIOLOGY

at the

CLEVELAND STATE UNIVERSITY

May, 2010

This thesis has been approved for
The Department of Biological, Geological,
And Environmental Sciences and the
College of Graduate Studies By

_____ Date: _____

Girish C. Shukla
Committee Chairperson, Department of BGES,
Cleveland State University

_____ Date: _____

Crystal M. Weyman
Department of BGES,
Cleveland State University

_____ Date: _____

Barsanjit Mazumder
Department of BGES,
Cleveland State University

ACKNOWLEDGEMENTS

Many people contributed their time, effort and ideas into completing this Master thesis; I would like to thank everyone who has helped me along the way.

First and foremost, I offer my sincerest gratitude to my advisor Dr. Girish Shukla for providing me an opportunity to conduct my research under his supervision. I was extraordinarily fortunate in having him as my undergraduate research professor. I could never have embarked and started all of this without his prior teaching. His sage advice, insightful criticisms and patient encouragement strongly contributed to the completion of this thesis.

Furthermore, I would like to record my gratitude to Dr. Crystal Weyman and Dr. Barsanjit Mazumder for their valuable advice and guidance from the early stage of my graduate career. Their teaching opened up unknown horizons to me. Also, I am thankful that in the midst of their tight schedule, they accepted to be members of my advisory committee.

I convey special acknowledgement to Dr. Bette Bonder for her indispensable help and support through the Graduate Assistantship. I am proud to record that I had several opportunities to work under Dr. Bonder's supervision in helping high school students throughout NEOSEF as well as CONSEF in designing and conducting experiment for their science fair activity.

I gratefully acknowledge Dr. Kavleen Sikand for her valuable advice in science discussion as well as giving me extraordinary experience throughout the work. Kavleen, your bright thoughts have been fruitful for shaping my ideas and knowledge.

I also would like to make a special reference to my colleague and friend Sanaa Jehi who patiently proofread this entire thesis. I have enjoyed our scientific discussions over the early morning coffee break.

I have worked with great number of people whom to I send a collective and individual acknowledgment, Neha, Tupa, Kevin, Megan, Jagjit and Chaucola. My lab colleagues whose presence perpetually was refreshing, helpful and memorable: Many thanks for giving me such a pleasant time.

This thesis is dedicated to my father Elias Slaibi and my mother Ghada Daura, their unswerving devotion to me is exemplified in many ways. You have raised me with caring and gentle love. You have implemented the fundament of my learning character, showing me the joy of intellectual pursuit ever since I was a child.

Mathilda, Natali and Slaibi, thanks for being supportive and caring siblings. This thesis will not be complete without the three of you.

Lastly, I offer my regards and blessings to all of those who supported me in any respect during the completion of the project.

TARGETS OF HSA-MIR-488* IN HUMAN PROSTATE CARCINOMA CELLS

JINANI ELIAS SLAIBI

ABSTRACT

Prostate cancer (PCa) is one of the most prevalent forms of cancer among men in America and is second only to lung cancer as a cause of cancer-related deaths in men. Recent epidemiological study shows that one in every six men over the age of forty five is at risk of PCa. Androgen receptor (AR) plays a causative role in the development of PCa. Hormonal blockade therapy which inhibits the expression of AR eventually fails and disease progresses to fatal androgen-refractory stage from androgen-dependent stage. Therefore, novel molecular approaches which can target and block the expression of AR are required. We propose that microRNAs (miRNA) that function as negative gene regulators have potential as PCa therapeutics. Using bioinformatics methods, we have identified that human miRNA hsa-miR-488* has potential to modulate AR expression. In the present study, we have validated the target site in AR 3'UTR and established that AR is a target of Hsa-miR-488*. Our data show that the ectopically expressed hsa-miR-488* as well as the synthetic miRNA mimic can suppress the expression of luciferase activity in chimeric plasmid harboring AR3'UTR with dose dependent effects. In addition, miR-488* negatively regulated the expression of endogenous androgen receptor in PCa cells LNCaP.

Thus hsa-miR-488* that function as negative gene regulators has potential as PCa therapeutics.

TABLE OF CONTENTS

	Page
ABSTRACT	V
LIST OF FIGURES	X
CHAPTER	
I. INTRODUCTION	
1.1 Cancer	1
1.2 Prostate cancer remains a significant public health problem in the U.S	3
1.3 Two stages of Prostate cancer	5
1.4 Mechanism of action of Androgen receptor	6
1.5 Regulatory noncoding microRNAs (miRNAs)	9
1.6 Relative genomic location of miRNA	11
1.7 microRNAs Processing	12
1.8 Hsa-mir-488* and Hypothesis	16
II. MATERIALS AND METHODS	
2.1 Cell Lines and Cell Culture	18
2.2 miRNA target validation	19
2.3 Cloning of 3' UTR AR in pMIR reporter Vector	20

2.4	Full length Mutated AR 3'UTR	22
2.5	Construction of vector expressed miR 488* "Pre-miR-488*"	24
2.6	Transient Transfection	24
2.7	RNA Extraction	27
2.8	Protein Extraction	27
2.9	Dual Luciferase assay	28
2.10	Quantitative Real-Time (qRT) PCR Analysis of Mature miRNA Expression	29
2.11	Statistical analysis	30

III. RESULTS AND DISCUSSION

3.1	Identifying potential target site for miR-488* in AR 3'UTR	32
3.2	Effect of miR-488* on AR expression	35
3.3	Target Validation: Construction of Luciferase Reporter Plasmids expressing AR 3'UTR	36
3.4	Target Validation: Effect of miR-488* mimic on the chimeric AR 3'UTR WT luciferase reporter plasmid	38
3.5	Base pair interaction between miR-488* and predicted target site	40
3.6	Cloning Shorter AR 3' UTR	43
3.7	Dose dependent expression of mature miR-488* from Pre-miR-488* expression plasmid	46
3.8	Dose dependent repression of Firefly luciferase	

expression by Pre-miR-488*	48
3.9 Mutations within miR-488* precursor in different cell lines	50
3.10 Stable cell line (LNCaP and C4-2B) expressing miR-488*	52
IV. FUTURE DIRECTIONS AND CONCLUSION	
4.1 Implication of the CG substitution in mature miR-488* processing	55
4.2 Identifying miR-488* precursor promoter	56
4.3 Library of miR-488* Target site	58
4.4 Conclusion	60
LITERATURE CITED	62
APPENDICES	68

LIST OF FIGURES

Figure		Page
Figure.1	2009 estimated US cancer deaths and cancer cases	4
Figure.2	Mechanism of action of Androgen receptor	7
Figure.3	microRNA processing model	14
Figure.4	miRNAs control gene expression	16
Figure.5	Astrotactin gene illustration	17
Figure.6	base pair alignment of AR3'UTR wild type and miR-488*	20
Figure.7	base pair alignment of AR3'UTR seed MUT and miR-488*	23
Figure.8	base pair alignment of AR3'UTR 5' MUT and miR-488*	23
Figure.9	Schematic representation of AR 3'UTR with the location of miR-488* predicted target site	33
Figure.10	Cluster alignment of AR 3'UTR of different species	34
Figure.11	Cluster alignment of precursor sequence of miR-488* in five different species	35
Figure.12	Effects of miR-488* mimic on AR protein expression	35
Figure.13	Restriction digestion clone confirmation	36
Figure.14	Quantitative analysis of the chimeric AR 3'UTR wild type luciferase plasmid repression by miR-488* mimic	38
Figure.15	Base pairing interaction between miR-488* and predicted target site	40

Figure.16 Effect of AR 3'UTR mutations on the levels of luciferase expression in the chimeric plasmid	42
Figure.17 miR-488* mutated mimic alignment with AR 3'UTR	44
Figure.18 Chimeric plasmid with Shorter AR 3'UTR can be targeted by miR-488*	45
Figure.19 Quantitative Real-Time (qRT) PCR analysis of mature miR-488* expression	46
Figure.20 Quantitative analysis of repression of luciferase sensor by Pre-miR-488* expression vector	49
Figure.21 Cluster alignment of miR-488* stem-loop region in different cell lines	51
Figure.22 Folding state of miR-488* stem loop	51
Figure.23 Stable cell line (LNCaP and C4-2B) expressing miR-488*	53
Figure.24 Schematic presentation of the genomic location of miR-488*	56
Figure.25 mini gene construct to check for independent promoter activity of miR-488*	57
Figure.26 Examples of miR-488* targets sites in 3'UTR of their perspective genes	58

CHAPTER I

INTRODUCTION

1.1 Cancer:

Human body is made up of about 100 trillion of living cells (Campbell, N.A. *et al.* 2006). Normal cells carry a complete organismic genome which is far more information that any cell may require (Sinden, R.R. 1994). Regulation of the cell cycle is critical for the development of multicellular organisms. Part of this information in normal cells controls essential function for the normal survivor of cells such as growth, dividing, and dying in an orderly way. However, cancer cells have lost the ability to control growth and division leading to uncontrolled proliferation and the inappropriate survival of damaged cells. This new fate of the uncontrolled cells is responsible for the formation of tumors.

Cells have developed several safeguards to ensure that cell division, differentiation and death occur correctly and in a coordinated fashion, both during development and in the adult body (Esquela-Kerscher A. et al., 2006). Mutations into this genomic information divert cells into acquiring novel or abnormal phenotypes and incompatible features with normal cell cycle. These mutations may cause inability of cells to make a functional signal, or cause it to code for a protein that sends an incorrect signal to the cell (Kinzler K.W. et al. 2002). Most mutations are repaired by the cell, but in rare cases mutations do not get repaired. If a mutation is not repaired before a cell copies its DNA and divides into two cells, then the mutation is passed on to the two new daughter cells and becomes permanent. Some genetic disorders may cause cells deprivation of their ability to repair DNA, and may therefore experience buildup of mutations. Not all the mutations within the cell's DNA have effect on whether the cell will become cancerous or not (Sawyer S.A. et al. 2007). However, protein signals coded by a very small proportion of the total genes in each cell regulate cell growth and division. These regulatory genes include the two groups of genes called Proto-oncogenes and tumor-suppressor (Chial, H. 2008). A series of mutations in the DNA of either and/or both groups of these growth controlling genes is selected in cancerous cells. Thus cancer is considered to be a genetic disease and the cancer-forming process is called Tumorigenesis or Oncogenesis, where most cancers may arise through a combination of avoidable or unavoidable carcinogens (Lutz W.K. et al, 1988).

Many factors contribute to the transformation of normal cells into malignant cancerous cells such as exposure to carcinogens, genetic defects, life style or even viruses (Couch D.B. 1996). Cancer cells have gained the ability to grow and multiply out of control forming a large mass of tissue called a tumor. Some tumors are limited to one location and can be surgically removed. These tumors do not grow in an unlimited, aggressive manner, do not invade surrounding tissues and do not metastasize. This type of tumors is termed benign tumor (Ramzi C.*et al.* 1999). But in other cases of cancer, cells have gained the ability to spread and metastasize to surrounding tissue or other organs of the body. Such aggressive tumors are termed malignant. The term cancer is used to describe malignant, non benign tumors.

1.2 Prostate cancer remains a significant public health problem in the U.S.

Prostate cancer is the most common solid tumor form of cancer among men in America and is second only to lung cancer as a cause of cancer-related mortality (Jemal A. *et al.* 2008, 2005 ; Parker S.L *et al.* 1997). Despite earlier diagnosis and improvement in treatment modalities, the cancer's projection for 2009 estimated that 192,280 new cases of prostate cancer will occur in the US during 2009 and 27,360 men will die from the disease (ACS, 2009).

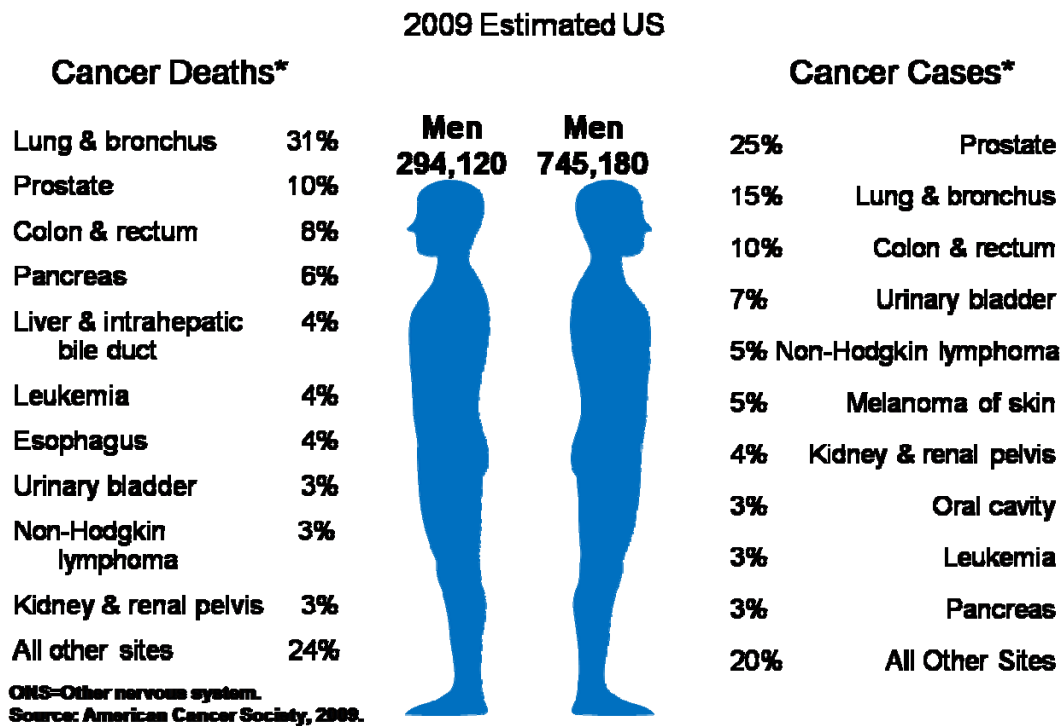


Figure 1: Statistical figures were adopted from the 2009 American cancer Society statistical study and rearranged in order to show the comparison between occurrence of cancer cases and the mortality rate of each site. Prostate cancer is the most diagnosed cancer within men and the second cause of cancer death in American men.

Numerous studies have shown that approximately 85% of newly diagnosed prostate cancer cases are localized in the prostate, and the remaining 15 % of the cases represents invasive or metastatic disease (Cooperberg MR *et al.* 2004). Those studies have provided insight into molecular mechanisms that contribute to the beginning and progression of prostate cancer. Most of these studies have suggested that androgens play an important role in the development, regulation and progression of prostate cancer. Hence, the first line for treatment is the Androgen deprivation therapy either surgical or chemical castration through a complete hormonal blockage of androgen by using anti-

androgens and in most cases combined with radiation in specific settings (Harries W. *et al*, 2009; Taneja S.S, 2003). While most patients with prostate cancer initially respond to androgen-ablation therapy, however 20% are refractory to such treatments. Furthermore, majority of the patients who respond to androgen ablation therapy eventually relapse with androgen-independent prostate cancer (AIPC) within three years (Calabro F. *et al*, 2007).

1.3 Two stages of Prostate cancer:

The ligand-activated transcription factor, androgen receptor (AR), plays a central role in the development and progression of prostate cancer in humans. AR is heterogeneously expressed in primary tumors and throughout the progression of androgen dependent and androgen independent 'hormone-refractory prostate cancers. Prostate cancer initiates as an androgen-dependent disease, and further accumulation of multiple sequential genetic and epigenetic alterations transforms it into an aggressive, therapy resistant, androgen-independent prostate cancer (AIPC) (Maitland J.N. *et al*, 2008).

The molecular basis of the transition from androgen dependent to AIPC is still unclear however; recent studies suggest that hypersensitivity of AR to trace level androgens combined with androgen ablation therapy could provide a selective pressure on the cellular pathways which are regulated by androgen signaling (Taplin, N.E *et al*, 1999; Craft N. *et al*, 1999). Consequently, androgen dependent cancer cells adapt to the androgen-deprived conditions and furthermore select

mutated AR that is able to utilize an anti-androgen antagonist as an agonist for their aggressive growth and proliferation (Marques, R.B *et al*, 2005).

Despite all the evidences, it is far from clear as to how AIPC arises and the definitive roles played by the AR.

1.4 Mechanism of action of Androgen receptor:

Prostate cancer is dependent on androgen stimulation mediated by the androgen receptor (AR). AR, a steroid hormone receptor member of the large nuclear receptor superfamily, is a ligand activated transcription factor that regulates the growth and the development of the normal prostate and plays a key role in the pathogenesis of prostate cancer (Balk S.P *et al.*, 2002; Quigley C.A *et al.*1995).

Androgens stimulate proliferation and inhibit apoptosis, thus maintain the ratio of proliferating cells to those dying. The maintenance of this ratio is very critical for the normal growth of prostate cells (Feldman B.J and Feldman D., 2001). Testosterone and dihydrotestosterone (DHT) are the major androgens in men. Testes produce over 90% of the hormone testosterone and the remaining small fraction 5-10 % is synthesized in the adrenal glands. The largest concentration of testosterone is circulating in the body, while most of the DHT's concentration is present in the prostatic tissues (Labrie FMD, 2004). About 75 % of DHT is produced by the prostate and the skin while the remaining 25 % circulating DHT is produced by the testes (Imamoto T. *et al.* 2008).

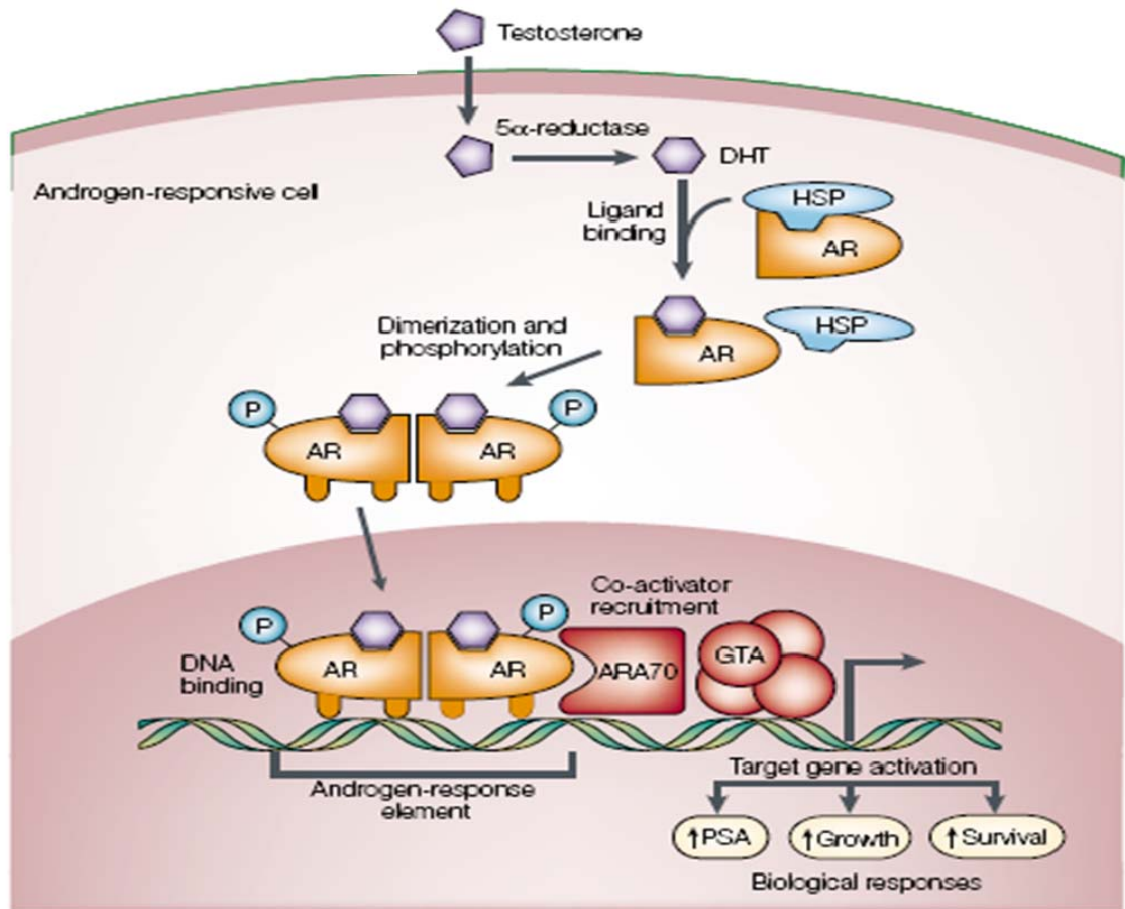


Figure 2: Mechanism of action of Androgen receptor: Testosterone enters cell membrane to the cytoplasm, where it is converted to DHT by 5 α -reductase enzyme (5 α R). In the presence of DHT, AR will dissociate from the HSP and bind to DHT, leading to conformational changes in the AR. Upon the phosphorylation of AR homodimer it enters the nucleus and binds to the genes containing the androgen response element, resulting in biological responses. Bartel et al 2004.

After being secreted by the testes, the testosterone hormone circulates in the blood flow. When it reaches the prostatic tissues, the testosterone enters the prostate cell membrane to the cytoplasm. In the cytoplasm, almost 90% of the testosterone is converted by 5 α -reductase enzyme (5 α R) to DHT. Dihydrotestosterone has much stimulatory effect on prostate cells growth

compared to testosterone and it has 5 fold higher affinities for AR than testosterone (Feldman and Feldman, 2001; Montgomery *et al* 2009).

Androgen receptor contains an N-terminal domain which is known as the regulatory domain and contains also two other domains: the first is a DNA binding domain (DBD) and the second is the ligand binding domain (LBD). In addition, AR has a hinge region that connects the Ligand binding domain to the DNA binding domain, followed by C-terminal domain (Brinkmann A.O., *et al* 1989).

In basal state, AR binds to the heat shock protein complex (HSP). This binding has the role of a chaperone to maintain the AR in a ligand-binding conformation (Balk S.P, 2002). In the presence of DHT, AR dissociates from the HSP and bind to DHT. This interaction leads to conformational changes in the AR and results in the formation of a homodimer which is phosphorylated by protein Kinase A (Feldman & Feldman, 2001; Balk S.P, 2002; Lynne V. *et al*, 1996).

Upon the dimerization and phosphorylation of androgen receptor, the newly formed complex enters the nucleus where it binds to the androgen response element in the promoter regions of the target gene (Chen C.Z *et al*, 2004). This binding will lead to the recruitment of co-activators and co-repressors which results in biological responses by triggering the translation process leading to up or down regulation of specific gene transcription (Feldman & Feldman, 2001; Balk S.P, 2002).

Up-regulation or activation of transcription results in increased synthesis of mRNA which in turn is transcribed by ribosomes to produce specific proteins. Thus a change in the levels of specific proteins in cells is one way by which androgen receptors control cell behavior.

1.5 Regulatory noncoding microRNAs (miRNAs):

MicroRNAs are a large family of phylogenetically conserved short, endogenous, single-stranded, 20-25 nucleotide long, noncoding RNAs molecules that can regulate gene expression in many different organisms ranging from viruses to plant to worm and humans (Lee R.C *et al*, 1993; Chen C.Z *et al.*, 2004; Pasquinelli A.E. *et al*, 2000) (Appendix: Table I and Figure I) . The best known founding members of this family are *lin-4* and *let-7* of *Caenorhabditis elegans* (Lee R.C *et al*, 1993; Pasquinelli A.E. *et al*, 2000). To date, more than 10,884 miRNAs have been annotated and 721 of these are human miRNAs. (miRbase, Release 14, Sep 2009). These numbers are likely to change when many more tissue specific miRNAs would be discovered by small RNA cloning and sequencing strategies. miRNAs regulate the expression of thousands of target mRNAs; each target mRNA has been predicted to be regulated by multiple miRNAs.

Computational analysis suggests that over 30% of human genes are regulated by miRNAs. Genes that are potentially targeted by these miRNAs include cell growth and maintenance, signal transduction, cell proliferation,

phosphorylation, cell cycle, transcription factors, cell organization and biogenesis (Nilsen T., 2007). In animals, miRNA mediates gene expression through translational repression of its target mRNA by binding at the 3' untranslated region (UTR) in imperfect complementarity (Wightman B. *et al*, 1991).

Many examples of documented miRNA functions were discovered in animals and include regulation of signaling pathways, apoptosis, metabolism, cardiogenesis and brain development (He L. and Hannon J., 2004).

miRNAs may play a critical role in the process of tumorigenesis since a deregulation of these biological processes are frequently occurred in human cancer (Wenyong Z., *et al.*, 2007). Evidence suggests that miRNAs can contribute to carcinogenesis by acting as tumor suppressors or oncogenes since they usually suppress the expression of oncogenes or proliferation related genes (Xu-Bao S., *et al.*, 2008). For instance, miR-15a and miR-16-1 are deleted or down-regulated in the majority of Chronic Lymphocytic Leukemia (CLL) and negatively regulate the antiapoptotic B cell lymphoma 2 (Bcl2) protein resulting in induced apoptosis in a leukemic cell line model. (Cimmino A., *et al.* 2005). Although many miRNAs are found to be significantly differentially expressed in different cancer types, to date, only a few have been well characterized for their functional significance.

1.6 Relative genomic location of miRNA:

Scientists identified three groups of miRNA genes based on genomic location relative to protein coding gene locus:

1. Intronic miRNA in protein coding transcription units (61%) e.g: *miR-10* in HOX4B gene (Lagos-Quintana *et al.*, 2003; Lim L.P *et al.*, 2003).
2. Intronic miRNA in noncoding transcription units (18%) e.g: *miR-15a-16-1* cluster found in the fourth intron of a previously defined noncoding RNA gene, DLEU2. (Narry K. and Jin-Wu N., 2006)
3. Exonic miRNA in noncoding transcription units (20%), such as *miR-155*. (Cai X. *et al*, 2004; Lee *et al.*, 2004).

MicroRNA genes are found in regions of the genome as separate transcriptional units as well as in clusters of polycistronic units coding for several miRNAs. It was found that approximately half of known miRNA exist in non-protein coding RNAs (intron and exon) or within the intron of protein coding genes (Erdmann, V.A., *et al.* 2004).

MicroRNAs that reside in introns share the same promoters and regulatory elements of their host gene (Sikand K. *et al.*, 2009) as for the other miRNA genes transcribed from their own promoters, few primary transcripts have been entirely identified (Lagos-Quintana M., *et al.*, 2001; Lau N.C. *et al.*, 2001).

Computational analysis suggested that 60% of protein encoding genes may be regulated by miRNAs. This fact suggests some important, yet undiscovered regulatory mechanisms linked to miRNAs. A significant number of miR genes (52.5%) are in cancer-associated genomic regions or fragile sites (FGA) (Calin G.A. *et al.*, 2004).

1.7 microRNAs Processing:

Little is known about transcriptional processes for miRNAs. It has been shown that miRNAs control gene expression by binding to the complementary sites in the 3' untranslated regions (3'UTRs) of target mRNAs and triggering therefore either translational inhibition or mRNA degradation by a molecular mechanism that is actively investigated (Wightman B. *et al*, 1991; Zamore D., 2005; Hutvagner & Zamore, 2002).

The majority of microRNAs are transcribed by RNA polymerase II from different genomic locations as long primary transcript of about 125 nucleotides in length, with a stem-loop structure known as (pri-miRNA) (Figure 3) (Lee *et al*, 2002; Cai X. *et a.l*, 2004; Kim V.N *et al.*, 2005). Initially it was thought that miRNAs are transcribed by RNA polymerase III (PolIII) (Cai X. *et al*, 2003), however some of the pri-miRNAs are several kilobases long hosting some stretches of more than 4 uracile nucleotides, which is unfavored by Pol III and will ultimately lead to the termination of transcription by Pol III (Lee Y. *et al.*, 2004). Recently it is believed that Pol II is responsible for transcribing the majority of miRNAs (Cai X. *et al*, 2004; Kim V.N *et al.*, 2005).

Subsequent to transcription in the nucleus, the pri-miRNAs are further processed by Drosha, RNase-III endonuclease. This enzyme belongs to the family of double stranded RNA specific ribonucleases (Cai X. *et al*, 2003). Drosha functions as a large protein complex called Microprocessor complex. This large nuclear protein complex (about 550 kDa) plays the role of pri-miRNAs metabolizing machinery. The Microprocessor is composed of the enzyme Drosha bound to a dsRNA-binding protein known as DGCR8 as well as many other splicing factors (Gregory R.I *et al*, 2004). Upon the processing of pri-miRNA by the Microprocessor complex, a shorter stem-loop shaped RNAs called precursor miRNA (Pre-miRNA) is formed, that is about 70 nt RNAs with 2-3 nucleotides 3' overhangs, 25-30 base pair stem containing multiple bulges and mismatches with relatively small loops (Lee Y. *et al*, 2003). Pre-miRNAs bearing a base-paired 5' end and 3' overhang of about 3 nucleotides are then transported to the cytoplasm by Exportin 5/RAN-GTP complex (Yi *et al*, 2003; Bohnsack *et al* 2004; Gwizdek *et al*, 2003).

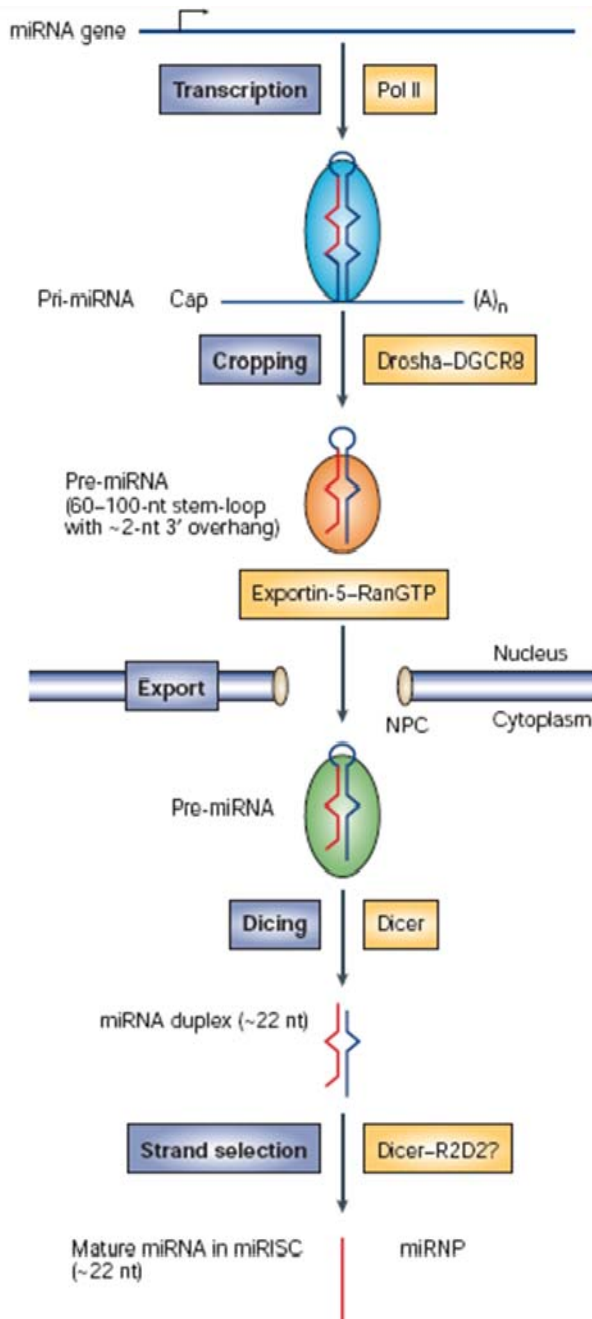


Figure 3: microRNA processing model:

microRNA (miRNA) genes are transcribed by RNA Polymerase II (Pol II) to form large pri-miRNA transcripts, which are capped and polyadenylated. These pri-miRNA transcripts are processed by the RNase III enzyme Drosha and its co-factor, to release the ~70-nucleotide pre-miRNA precursor product. RAN-GTP and exportin 5 transport the pre-miRNA into the cytoplasm. Subsequently, another RNase III enzyme, Dicer, processes the pre-miRNA to generate a transient ~22-nucleotide miRNA:miRNA* which will eventually result in mature single stranded miRNA (Lee Y. *et al*, 2003).

In the cytoplasm, pre-miRNAs are cleaved by Dicer, cytoplasmic RNase III-type enzyme. Dicer contains two RNase III domains, each domain cuts independently one RNA strand of the pre-miRNA complex yielding a product of about 22 nucleotides in length with 2-3 nucleotides overhang, during this process the duplex is unwound by unknown helicase-like enzyme (Kolb F.A. *et al*, 2005). Subsequently one strand dicer cleaved pre-miRNAs called the mature miRNA is incorporated into effector complexes that are known as 'miRISC' (miRNA-containing RNA-induced silencing complex) (Hutvagner and Zamore , 2002). miRISC complex delivers mature miRNA to its target mRNA through base pairing with the 3' untranslated regions (UTR) (Bartel D.P *et al.*, 2004).

miRNAs control gene expression by binding to the complementary sites in the 3' untranslated regions (3' UTRs) of target mRNAs (Figure 4), however, the target sequence inserted into the 5'UTR or the coding sequences are also functional (Kloosterman W. *et al*, 2004). If the miRNA has perfect or near-perfect complementarity to the 3'UTR of target mRNA, it will result in mRNA degradations (Figure 4 A) (Hutvagner & Zamore 2002; Bartel D.P *et al.*, 2004). On the other hand, the presence of multiple mismatches between miRNA sequence and mRNA of target site, leads to translational inhibition without affecting mRNA levels of target site (Figure 4 B) (Bartel D.P *et al.*, 2004). Molecular mechanism underlying either miRNAs mRNA mediated degradation or miRNAs mediated translation repression are not fully understood, thus both mechanisms are subject of intense investigation.

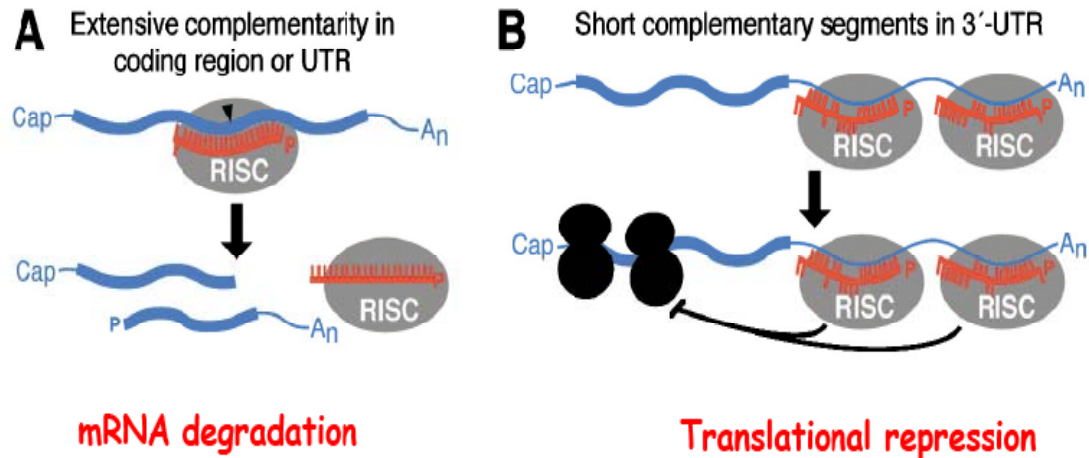


Figure 4: miRNAs control gene expression: MiRNAs that bind to their mRNA targets with perfect complementarity induce target-mRNA cleavage Panel A. The mature miRNA binds to complementary sites in the mRNA target to regulate gene expression in one of two ways, miRNAs that bind to mRNA targets with imperfect complementarity block target gene expression at the level of protein translation Panel B.

1.8 Hsa-mir-488* and Hypothesis:

Recent studies reported that some miRNAs might play an important role in prostate cancer by targeting the expression of some growth regulatory genes. These miRNAs include miR-15 (Bonci D. *et al*, 2008), miR-101 (Varambally S. *et al*, 2008), miR-125b (Lee C.Y. *et al*, 2005), miR-221 (Folini M. *et al.*, 2009). Unexpectedly, no miRNA yet to date has been reported to regulate androgen receptor in prostate cancer, despite the fact that androgen receptor ablation has been found to inhibit cell proliferation, thus demonstrating the essential functional role of AR in the growth of prostate cancer cells. We hypothesized that miRNAs may be involved in the regulation of androgen receptor signaling and these miRNA could be used for targeting androgen receptor in prostate cancer. Using

computational analyses, we identified a potential target site for hsa-miR-488* in the 3' untranslated region of androgen receptor mRNA.

Hsa-miR-488* encoded in intron 5 of Astrotactin 1 (ASTN1) gene (Figure 5).

Astrotactin is a neuronal adhesion molecule required for glial-guided migration of young postmitotic neuroblasts in cortical regions of developing brain, including cerebrum, hippocampus, cerebellum, and olfactory bulb (Flink *et al*, 1995).

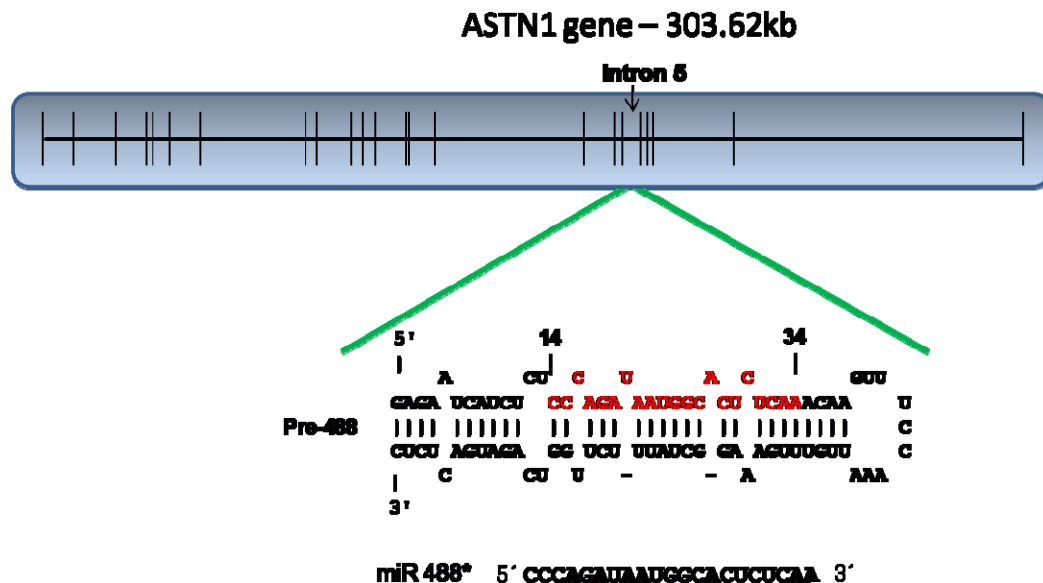


Figure 5: Astrotactin gene host the intronic region that code for Hsa-mir-488*. Hsa-mir-488* encoded in intron 5 of the ASTN 1 gene.

This work investigated the methods to validate miR-488* target site in the proposed gene (AR). What are some of the effect of miR-488* on its targets in prostate cancer cells, and could this technique be used on different target sites?

CHAPTER II

MATERIALS AND METHODS

2.1 Cell Lines and Cell Culture:

LNCaP:

The androgen-dependent human prostate carcinoma cell line LNCaP, was obtained from American Type Culture Collection ATCC (Manassas, VA). LNCaP cells were cultured in appropriate cell culture grade plates with 1X RPMI 1640 medium supplemented with 10% Fetal bovine serum (FBS) Atlanta Biologicals, Inc. (Lawrenceville, GA) 2mM L-glutamine and antibiotics (100 units/ml of penicillin G sodium, 100µg/ml streptomycin sulphate). LNCaP cell lines were maintained in a humidified 5% CO₂ at 37°C.

CHO:

Chinese Hamster Ovary cell line CHO, was obtained from American Type Culture Collection (Manassas, VA). CHO cells were cultured either in 6 well or 24 well plates with 2 ml or 500µl of Dulbecco's Modified Eagle's Medium (DMEM) respectively, supplemented with 2 mM L-glutamine, 4.5 g/l Glucose, 5% Fetal bovine serum (FBS) Atlanta Biologicals, Inc. (Lawrenceville, GA), 1 mM L-proline, 10mM HEPES and antibiotics (100 units/ml of penicillin G sodium; 100µg/ml streptomycin sulphate). Trypsin 1X was added up to 2 ml of cells and incubated at room temperature for 3 minutes. Trypsin 1X was quenched with 3 ml of DMEM 1X supplemented with 5% FBS, 1mM L-proline, 10 mM HEPES and antibiotics. Cells were finally seeded at an approximate density of 3.0×10^4 cells/well for 24 well plates and 1.0×10^5 cells/well for 6 well plates. All cell lines were maintained in a humidified 5% CO₂ at 37°C.

2.2 miRNA target validation:

miRNA is an emerging field of science and the knowledge about miRNAs target still limited. Researcher in the field of miRNA combined computer algorithms with biological information after the establishment of the human genome to identify and predict target site for miRNAs. This new field of science is called bioinformatic in our lab we have used bioinformatic *methods*, to identify miRNAs which can potentially bind to the 3' UTR of the AR. Several miRNAs target prediction tools such as TargeSCAN, MirSCAN, Find TAR and RNAhybrid have identified that hsa-mir-488* could potentially base-pair with the 3' UTR of

the androgen receptor. Hsa-mir-488* has extended base-pair matching sequence to the seed region of the predicted site 10 nucleotide and minimal none Watsoncrick base paring (1 G: U). Overall hsa-mir-488* has 80% complementarities to the predicted target site suggesting that AR 3'UTR could be targeted by hsa-mir-488* (Figure 6).

RNAhybrid – Results (QueryID: bibiserv_1269872147_3730)



Figure 6: base pair alignment of AR3'UTR wild type and miR-488*: seed region consist of 10 base pair with perfect complementarity, straight line (|) represent Watsoncrick base paring, and (:) represent G:U non watsoncrick interaction.

2.3 Cloning of 3' UTR AR in pMIR reporter Vector:

Full length wild type AR 3'UTR:

Primer name	Primer sequence
AR 3' UTR forward	5'-GCGCA <u>CTAGT</u> ACGTTTACTTATCTTATGCCACGGG-3' Spel site
AR 3'UTR reverse	5'-GCGCA <u>AAGCTT</u> GTGGCTTGTGGTTTGTGGTTTGTGGTTTTC-3' HindIII site

For the construction of AR 3' UTR reporter plasmid, two primers (table 1) AR 3' UTR forward and AR 3'UTR reverse were designed to introduce SpeI and HindIII sites (underlined) at the end of PCR product of 637 bases fragment of AR 3'UTR spanning the predicted target site for hsa-miR 488* (Appendix, Fig 2) .

Thermodynamic analysis of the primers was conducted using computer program: Primer Express (Applied Biosystems, Foster City, CA). The resulting primer sets were compared against the entire human genome using NCBI to confirm specificity and ensure that the primers flanked hsa-mir-488* target site on the androgen receptor 3'UTR.

AR 3'UTR with both restriction sites was amplified through PCR technique using the following PCR conditions.

PCR conditions:

Reagent	Volume	Stock
5X Buffer	10µl	5x
Mgcl ₂	5µl	25 mM
dNTP	1µl	10 mM
PCR water	30.5µl	
AR 3'UTR forward Primer	0.5µl	10 µM
AR 3'UTR reverse Primer	0.5µl	10 µM
Taq polymerase enzyme	0.5µl	5 units/µl
human gDNA	2 µl	50ng/µl

Optimized Thermocycler Parameters:

1. 95 °C 2 minutes
2. 95 °C 1minute
3. 55 °C 1minute
4. 72 °C 30 sec (go to 2 x 30 times)
5. 72 °C 10minutes
6. 4 °C 4hours

The resulted PCR product purified and concentrated using ZYMO research DNA clean & concentrator™-25 kit (ZYMO, Orange, CA) following the manufactory protocol. After restriction digestion with SpeI and HindIII enzyme, the amplified DNA was cloned into the corresponding sites of pMIR-REPORT vector (Ambion, Austin, TX) downstream of firefly luciferase gene. The resulting plasmid construct WT-3'UTR contains a strong CMV promoter driving a luciferase expression cassette (Appendix, Fig 3).

2.4 Full length Mutated AR 3'UTR:

Site-directed mutagenesis of the putative target site for hsa-miR-488* in WT-3'UTR construct was carried out in order to generate the MUT-3'UTR constructs using the Change-IT Multiple Mutation Site Directed Mutagenesis kit (USB Corporation, Cleveland, OH). In the first MUT-3'UTR construct, 10 nucleotides in the seed matching region of the target site were mutated to their complementary nucleotides using primer

5'Phosphate group
CTTATGCCACGGGAAGAAACTCTCACGGAAGATTATCTGGGGAAAT

The newly generated construct was named AR 3'UTR seed MUT (Figure 7)

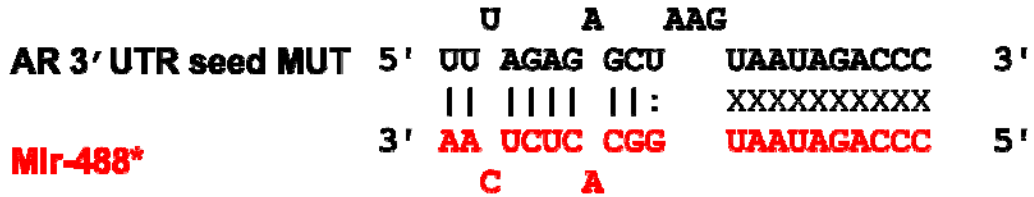


Figure 7: base pair alignment of AR3'UTR seed MUT and miR-488*: mutations introduce to the first 10 nt of the predicted target site (X) represent no interaction (|) represent Watsoncrick base paring, and (:) represent G:U non watsoncrick interaction.

The second primer was designed to mutate the 5' half of the putative miR-488* site of the AR 3'UTR (Figure 8).

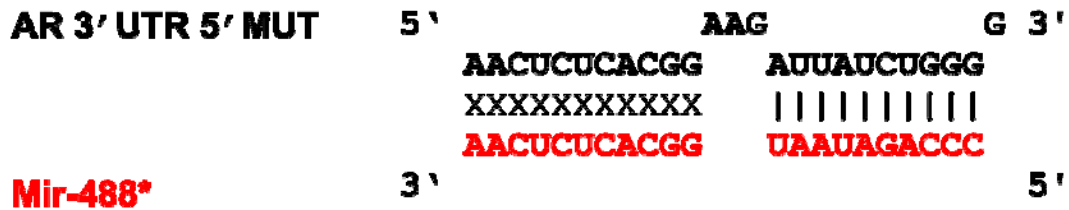


Figure 8: base pair alignment of AR3'UTR 5' MUT and miR-488*: mutations introduce to the 5' half of the predicted target site (X) represent no interaction (|) represent Watsoncrick base paring.

Both of the mutated constructs AR3'UTR seed MUT and AR3'UTR 5'MUT, as well as a new construct combining both mutations on the same backbone were generated following Change-IT Multiple Mutation Site Directed Mutagenesis kit manufacturer protocol. Nucleotide sequences of the constructs were confirmed by DNA sequencing.

2.5 Construction of vector expressed miR 488* “Pre-miR-488*”:

Segment of 383bp from intron 5 of ASTN 1 gene harboring the precursore sequence of miR 488* along with a flanking region was amplified from human genomic DNA using the following primers carrying XhoI and BamHI sites (Table 3).

Primer name	Primer sequence
Pre-488* forward	5'- GCACCTCGAGTGGGAGTGAGGGAGGCGGGGGAAG-3' XhoI
Pre-488* reverse	5'- GCACGGATCCCCCCAATCCTTGCCTAGCTCAAAC-3' BamHI

The XhoI-BamHI digested amplified DNA was cloned into the corresponding sites in pcDNA 3.1 (-) vector (Invitrogen, Carlsbad, CA). This construct was named Pre-miR 488*. The primer validation and cloning method were performed as for previous construct (Appendix, Fig 6).

2.6 Transient Transfection:

Equal cell numbers (3.0×10^4 cells/well for 24 well plate and 1.0×10^5 cells/well for 6 well plates) were seeded twenty four hours prior to transfection in DMEM 1x Supplemented with 2mM L-glutamine, 4.5 g/l Glucose, 5% Fetal

bovine serum (FBS) Atlanta Biologicals, Inc. (Lawrenceville, GA), 1mM L-proline, 10mM HEPES, but no antibiotics. Two Transfection procedures have been used:

Transfection via lipofectamine 2000:

This method was used with all transfections with miRNA mimic in 24 well plates. Two separate solutions were prepared as following:

- Solution I: In an Eppendorf tube, 0.75 μ l of lipofectamin 2000/well was added to 50 μ l of free serum free P/S CHO media. After gentle mixing through pipetting, the solution was incubated at room temperature for 5 min.
- Solution II: In an Eppendorf tube, 100 ng of AR 3'UTR firefly luciferase reporter construct was added to 50 μ l of free serum free P/S CHO media and then mixed with 0.5 ng of Renilla luciferase reporter plasmid. Finally, 10 nM of miR-488* mimic was added to the mixture. A Negative Control for the microRNA (NC mimic) was also prepared by adding 10nM of NC mimic to the mixture instead of miR-488* mimic.

Solution I and Solution II were mixed gently three to four times by pipetting and then incubated at Room temperature for 20 minutes.

The total volume of 100 μ l of Transfection mixture (Solution I + Solution II) was added drop by drop to the corresponding labeled wells which already contain 500 μ l of DMEM 1X supplemented with 2 mM L-glutamine, 4.5 g/l Glucose, 5% Fetal bovine serum (FBS) Atlanta Biologicals, Inc. (Lawrenceville, GA), 1mM L-

proline, 10mM HEPES, but no antibiotics . The 24 well transfected plate was incubated in a humidified 5% CO₂ incubator at 37°C for 48 hours.

Transfection via polyBrene:

This method was used to transfect CHO cells with Pre-miR-488* construct in 24 well plates. In an Eppendorf tube, 1.5 µl of PolyBrene 10µg/µl was added to 500µl of free P/S CHO media. After mixing the required amount of PolyBrene and free P/s media, the required concentrations of Pre-miR-488* was added. 100 ng of AR 3'UTR firefly luciferase reporter construct was added to the previous solution and then mixed with 0.5ng of Renilla luciferase reporter plasmid. Finally the mixture was incubated at room temperature for 5 min. Meanwhile the CHO medium was aspirated from the wells and the previously prepared transfection mixture was added to the designated wells. For the followed eight hours, the transfected plates were maintained in a humidified 5% CO₂ atmosphere at 37°C incubator with gentle swirling every one hour. Eight hours later, the Transfection media was aspirated out of the wells and the DMSO (Dimethyl Sulfoxide) shock was performed by adding 500 µl of 30% DMSO/ CHO media. The cells were incubated in the Shock medium at room temperature for 5 minutes. A washing step using 500 µl of CHO complete media was done, and then another 500µl of freshly prepared CHO media was added to each well. Finally, the transfected plates were maintained in a humidified 5% CO₂ atmosphere at 37°C incubator for forty eight hours from DMSO shock point.

2.7 RNA Extraction:

Total RNA from experimental and control wells were isolated from 80% confluent cells directly in the 6 well culture plate. Cells were homogenized in the culture dish and lysed directly by adding 1 ml of TRIZOL® Reagent (Invitrogen, Carlsbad, CA) following manufacturer's protocol. The cell lysate was collected in 1.5 ml Eppendorf tube. Samples were treated with chloroform, incubated at room temperature for 2 to 3 minutes and centrifuged (12,000 x rpm) for 15 minutes at 4 °C. The upper aqueous phase (approximately 450µl) was transferred to a fresh tube and precipitated by adding 1 volume of isopropanol to extract RNA. After 10 minutes of incubation at room temperature, RNA pellet was collected by centrifugation (12,000 rpm) for 10 minutes at 4° C. After discarding the supernatant, RNA pellets were washed with 1 ml 75% ethanol/ DEPC water and precipitated by centrifugation (12,000 rpm) for 5 minutes at 4°C. Pellets were resuspended in 50 µl of Rnase-free water. RNA yield and purity were determined spectrophotometrically at 260-280nm and the reliability of RNA was verified by electrophoresis through 1 % denaturing agarose gels stained with ethidium bromide.

2.8 Protein Extraction:

Additional wells containing experimental and control CHO cells were seeded for protein extraction. Cells were washed once with 500 µl cold PBS in 24 well plates. 100 µl of 1X passive lysis Buffer (PLB) was added and the culture

dish was gently rocked for 45 minutes at RT, then homogenized materials were collected in microcentrifuge tubes. Slow centrifugation at 4000 rpm for 15 minutes at 4° C was performed to pellet down any unlysed cells. The Protein quantification was determined by spectrophotometry at 595 nm and using 1X Bradford reagent (Bio-Rad Hercules, CA). The total protein concentration was calculated. Total protein lysates were stored at -80° C for further experimentation procedures.

2.9 Dual Luciferase assay:

For Dual luciferase assays, CHO cells (30,000 cells/ well) were plated in 24-well plates one day prior to transfection. Cells were co-transfected using lipofectamine 2000 reagent (Invitrogen, Carlsbad, CA), with 100 ng of WT-3'UTR or MUT-3'UTR firefly luciferase reporter construct, 0.5 ng of renilla luciferase reporter plasmid and either miR 488* mimic (10 nM) or NC mimic (10 nM). Cells were harvested and total protein concentrations were determined by Bradford method 48 hours after transfection. 10 µg of total cell protein lysates were assayed for firefly and Renilla luciferase activities using the Dual-Luciferase Reporter Assay System (Promega, Madison, WI) and Victor 3 Multilabel Counter 1420 (PerkinElmer). Aliquots of 10 µg of total cell protein lysates were transferred into oblique 96 well plates and 100 µl of LAR II reagent (Promega, Madison, WI) was dispensed into each well followed by orbital shaking for 2 seconds and incubation time of another 2 seconds, then 10 seconds of measurement of the emission light produced from the fire fly luciferase. Reading was recorded

electronically. In order to quench the emitted light from the firefly luciferase and to activate the emission of light from Renilla luciferase, 100 μ l of Stop & Glo® reagent (Promega, Madison, WI) was added to the previous wells, followed as before by 2 second of orbital shaking and 2 second of incubation time, then 10 second of measurement of emission of light produced by Renilla luciferase. Readings were recorded electronically. The whole procedure was carried out at room temperature.

2.10 Quantitative Real-Time (qRT) PCR Analysis of Mature miRNA

Expression:

From 10 ng of total RNA the first strand cDNA was synthesized using primers specific for miR-488* and snoRNA 202. Both primers were obtained from TaqMan MicroRNA Assays (Applied Biosystems Foster City, CA). Reagents for cDNA synthesis were obtained from TaqMan MicroRNA Reverse Transcription kit (Applied Biosystems). For each sample, a 15 μ l reverse transcription (RT) reaction was set up containing 10ng of total RNA, 1X RT buffer, 1mM of dNTP mix, 50 units of MultiScribe reverse transcriptase, 3.8 units of RNase inhibitor and 3 μ l of miRNA-specific RT primer. The reactions were incubated in a thermal cycler (BIORAD PTC-100) at 16°C for 30 minutes, 42° C for 30 minutes, 85° C for 5 minutes and then held at 4°C. The 'reverse transcriptase minus' controls were also synthesized under the same conditions. In order to quantify the mature miRNAs and snoRNA 202 in each sample, the cDNAs were amplified using TaqMan MicroRNA Assays together with the TaqMan 2X Universal PCR Master

Mix (Applied Biosystems Foster City, CA). For this step, a 20 μ l reaction was set up containing 1.33 μ l product from RT reaction, 1 μ l of 20X TaqMan microRNA assay mix (mixture of miRNA-specific forward and reverse primers, and miRNA-specific TaqMan MGB probe labeled with FAM fluorescent dye) and 10 μ l of TaqMan 2X Universal PCR Master Mix. These reactions were dispensed into a 96 well optical plate (Applied Biosystems Foster City, Ca). The plate was centrifuged at 2000 rpm for 5 minutes to remove any air bubbles that might be formed. After insuring the absence of air bubbles, the plate was positioned in 7500 Real-time PCR System (Applied Biosystems) under the following conditions: 95°C for 10 minutes followed by 50 cycles of 95°C for 15 seconds and 60°C for 1 minute. Three replicates were performed per RT reaction together with the 'reverse transcriptase minus' and 'no template' controls. Duplicate PCRs were performed for all miRNAs in each RNA sample. The mean C_t was determined from the replicates. The snoRNA 202 expression was used as an invariant control. The relative expression of each miRNA was calculated as $2^{-\Delta C_t}$ where $\Delta C_t = C_t$ value of each miRNA in a sample – C_t value of snoRNA 202 in that sample. All experiments were repeated at least twice with three replicates and two independent RNA samples (Appendix, Fig 7).

2.11 Statistical analysis:

To interpret our results, significance tests and statistical analysis are critical. The traditional α -value, i.e., $p = 0.05$, was used to evaluate the statistical significance of this study. The data of the dual luciferase and q-RT-PCR assays

results will be expressed as the mean \pm SEM and compared using student's *t*-test for normally distributed samples. The results were analyzed using the MYSTAT 12 version 12.02.00 statistical program (Systat Software, Inc.Chicago, IL) and Microsoft Excel (Microsoft, Seattle, WA). The index of expression of each miRNA was $2^{-\Delta Ct}$ after normalization to snoRNA 202 expression levels. Hence, results were considered statistically significant if *p* values were < 0.05 .

CHAPTER III

RESULTS and DISCUSSION

3.1 Identifying potential target site for miR-488* in AR 3'UTR:

Androgen receptor (AR) plays a central role in the development and progression of prostate cancer in humans. AR is heterogeneously expressed in primary tumors and throughout the progression of androgen dependent and androgen independent “hormone-refractory prostate cancers”. Prostate cancer initiates as an androgen-dependent disease, and further accumulation of multiple sequential genetic and epigenetic alterations transform it into an aggressive, therapy resistant, androgen-independent prostate cancer (AIPC).

The molecular basis of the transition from androgen dependent to AIPC is still unclear however; recent studies suggest that hypersensitivity of AR to trace level androgens combined with androgen ablation therapy could provide a selective pressure on the cellular pathways which are regulated by androgen signaling

(Taplin, N.E *et al*, 1999; Craft N. *et al*, 1999). Consequently, androgen dependent cancer cells adapt to the androgen-deprived conditions and furthermore select mutated AR that is able to utilize an anti-androgen antagonist as an agonist for their aggressive growth and proliferation (Marques, R.B *et al*, 2005).

MicroRNAs molecules can regulate gene expression in many different organisms by functioning as negative gene regulators (lee *et al*, 1993; lee and Ambrose, 2001; Bartel, 2004; Pasquinelli *et al*, 2000). In order to study the effect

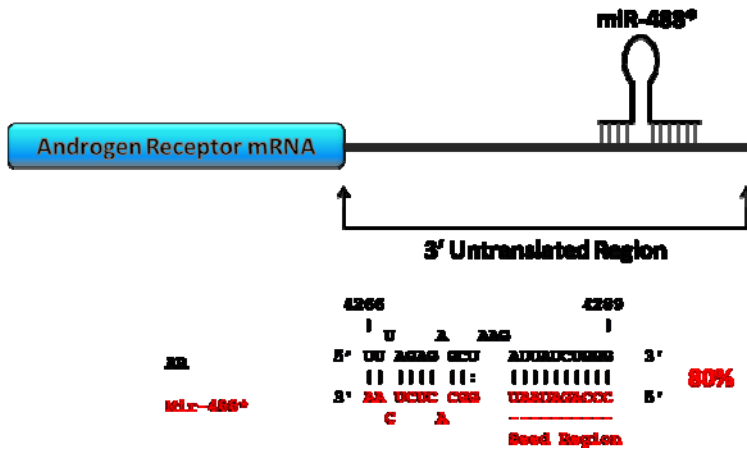


Figure 9: Schematic representation of AR 3'UTR with the location of miR-488* predicted target site: Hsa-miR-488* has extended seed region complementarity to the predicted target site (10 bases), followed by three bulges, resulting in 80% complementarity to the target site, according to Bartel et. al this such interaction should result in translation repression but not mRNA

of miRNAs on AR, we had to identify one miRNA that has the potential to bind to the 3' untranslated region of androgen receptor. Bioinformatic programs such as TargetSCAN, MirSCAN, Find TAR and RNAhybrid aided in accomplishing this task

by predicting one target site in the AR 3'UTR.

Our bioinformatics results indicated that hsa-mir-488* has target site in the 3' UTR of AR. Base pair interaction between the predicted target site and hsa-mir-488* is shown in (Figure 9).

Furthermore, bioinformatics approaches showed that the predicted target site is evolutionary conserved across different species (Figure 10). Those similarities

```

Human      ACTTATCTTATGCCACGGGAAGTTTAGAGAGCTAAGATTATCT--GGGAAAATCAAA-AC
Orangutan  ACTTATCTTATGCCACGGGAAGTTTAGAGAGCTAAGATTATCT--GGGAAAATCAAA-AC
Rat        ACTCACCTTATGCCATGGCAAGTTTAGAGAGCTATAAGTATCTTGGGAGAAACAAACAG
Pig        ACTCACCTAATGCCACGTGAAGTTTAGAGAGCTAAGAGTATCT--GGA
Cow        ACTCACCTAATGCCACGTGAAGTTTAGAGAGCTAAGAGTATCT--GGA AAA-CAAA-AG
*****

```

Figure 10: Cluster alignment of AR 3'UTR of different species: Sequence alignment of the miR-488* putative predicted target site in the AR 3'UTR of five different species: Target site boxed in green and stars indicate the conservation across all five species.

in sequence alignment serve as evidence for structural and functional conservation, thus this predicted site might have an important function within the development of these species.

In addition, precursor sequence for hsa-miR-488* encoded in intron 5 of Astrotactin 1 (ASTN1) gene in human is also highly conserved in five species (Figure 11). This is a further evidence that miR-488* has an evolutionary conserved role within the lineage of evolution. This extensive conservation strongly indicates a more general role for hsa-miR-488* in developmental regulation, as well as the predicted target site to be an authentic target site.

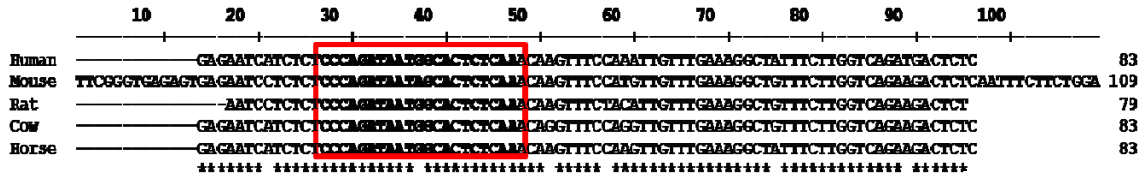


Figure 11: Cluster alignment of precursor sequence of miR-488* in five different species: Sequence alignment of pre-miR-488* in five different species, miR-488* mature sequence in red box. Stars indicate the conserved nucleotides.

3.2 Effect of miR-488* on AR expression:

In order to experimentally test the potential of miR-488* to regulate the

expression of AR, my lab

colleague Dr. Sikand

transfected PCa

Hormone dependent cell

line (LNCaP) with miR-

488* mimic or negative

control (NC), negative

control being a miRNA

from *C. elegans* that

has no target site in

human genome. After 48

hours of transfection,

cells were collected and

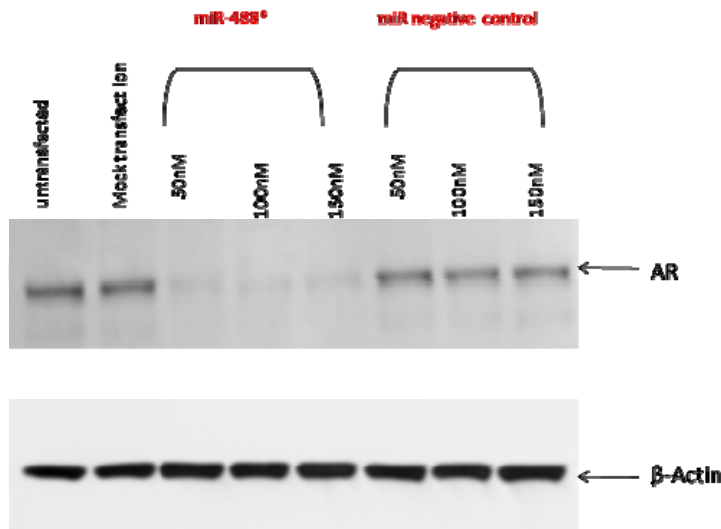


Figure 12: Effects of miR-488* mimic on AR protein expression: LNCaP cells were transfected with either miR-488* or NC mimic with the appropriate controls, cells were collected after 48 hours, total protein estimation was performed followed by western blot analysis. Results indicate high reduction of AR protein levels when transfected with miR-488* mimic compared to cells transfected with either NC mimic or mock transfected.

total protein amount was estimated, then a western blot was performed in order

to determine the AR protein expression. β-Actin was used as an internal control.

Results are shown in (Figure 12): when cells were transfected with different concentration of miR-488* mimic, a high reduction of AR protein levels was observed comparing to the cells transfected with the same concentrations of negative control miR mimic. In addition, negative control mimic had no effect on the AR levels compared to no transfection or mock transfection, which clearly indicates that the change in AR protein levels is due to the effect of miR-488* on the expression levels of Androgen receptor protein. Transient transfection of miR 488* mimic resulted in robust suppression of AR protein expression in LNCaP cells.

3.3 Target Validation: Construction of Luciferase Reporter Plasmids expressing AR 3'UTR.

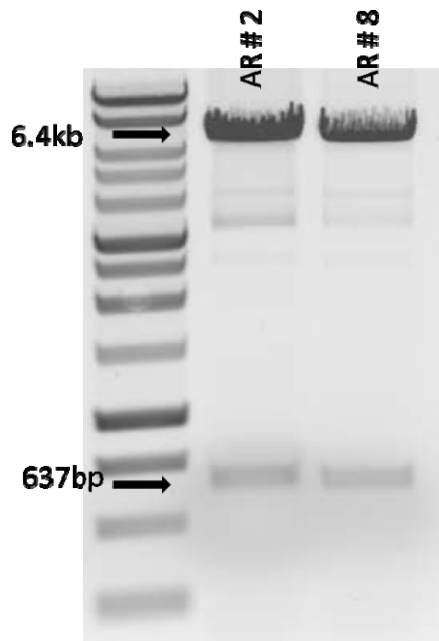


Figure 13: Restriction digestion clone confirmation: AR 3'UTR clone was confirmed by double digestion with SpeI and HindIII enzyme and analyzed on 1 % agarose gel.

In order to validate the previously observed data, we have to demonstrate that the repression of AR protein is due to the interaction between the predicted AR mRNA target site and miR-488*. To address this question, we cloned the AR 3'UTR containing the putative wild type miR-488* target site into the 3' multiple-cloning-site (MCS) of pMIR-REPORT vector (Ambion, Austin, TX) downstream of firefly luciferase gene as described in the "materials and method" section. The resulting plasmid construct WT-3'UTR contains a strong CMV promoter driving a luciferase

expression cassette (Appendix, Fig 3). The resulted clones first were confirmed by double digestion with SpeI and HindIII enzyme and analyzed on 1 % agarose 1X TAE gel and compared to 1 Kb ladder (Figure 13). As expected, a fragment of 637 base pair product was observed in two clones (clone #2 and clone # 8) indicating that AR 3'UTR was cloned successfully into the MCS of pMIR-REPORT. For further confirmation, the resulted clones were sequenced in the Cleveland clinic foundation genomic core facility, and once again the sequence result proved that indeed the cloned fragment is the AR 3'UTR.

3.4 Target Validation: Effect of miR-488* mimic on the chimeric AR 3'UTR WT luciferase reporter plasmid:

To address if miR-488* could target the AR 3'UTR, we have transfected the resulted chimeric sensor plasmid along with Renilla luciferase plasmid and the appropriate controls as described in the materials and method section into 80 % overnight grown CHO cells in the absence of antibiotics using lipofectamine 2000 as transfection reagent of choice. After 48 hours post

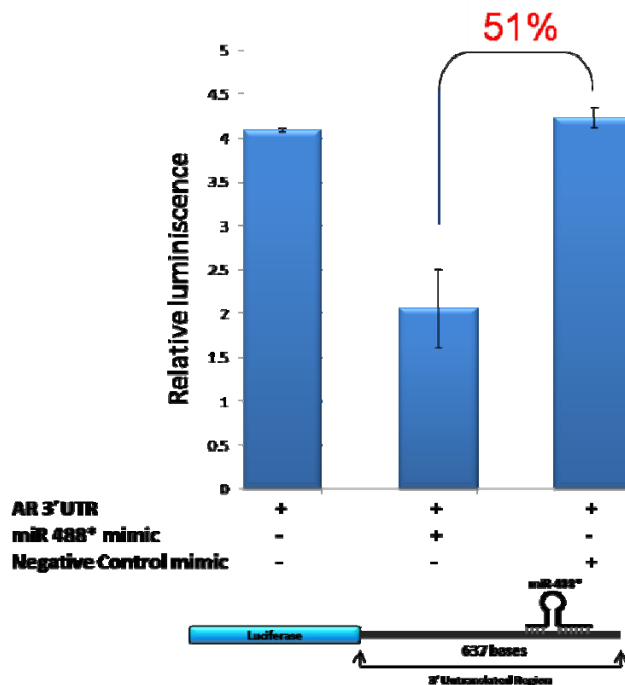


Figure 14: Quantitative analysis of the chimeric AR 3'UTR wild type luciferase plasmid repression by miR-488* mimic: CHO cells were cotransfected with chimeric AR 3'UTR luciferase reporter plasmid along with Renilla luciferase plasmid and miR-488* mimic (10nM) or NC mimic (10nM) are indicated. Down regulation of 51% of the firefly luciferase when transfected with miR-488* mimic was observed compared to transfection with NC.

transfection, cells were collected, washed once with 1X PBS and lysed in 1X PLB. Total protein was estimated using Bradford reagent and 10 µg of total protein was loaded into the designated wells of the 96 well plates. Protein lysates were assayed for firefly and Renilla luciferase activities using the Dual-Luciferase Reporter Assay System (Promega, Madison, WI) and Victor 3 Multilabel Counter 1420 (PerkinElmer).

Results showed that the transfection of miR-488* along with chimeric sensor plasmid (AR 3'UTR) resulted in down regulation of about 51% comparing to transfection with negative control of the same concentrations. This result indicates that miR-488* might be interacting and negatively down regulating the AR 3'UTR chimeric plasmid. However we are certain that this result is due to the interaction of miR-488* with the predicted target site and not with the body of pmiR REPORT, since no down regulation was observed when pmiR REPORT empty vector was transfected with the same concentration of miR-488* mimic and NC mimic. Furthermore none of the microRNAs target prediction tools have shown any target site for miR-488* in the empty pMIR report vector.

3.5 Base pair interaction between miR-488* and predicted target site:

MicroRNAs mediate gene expression through translational repression of its target mRNA by binding to the 3' untranslated region (UTR) in imperfect complementarity (Wightman B. *et al*, 1991; Bartel, 2004). MiR-488* has 80% complementarity to the predicted site, thus it is believed to bind to the predicted target site and through an ambiguous and not fully understood mechanism, drive an expression repression of its target gene (Nilsen T, 2007). To validate if miR-

◆ **Base pair interaction between miR-488* and predicted target site**

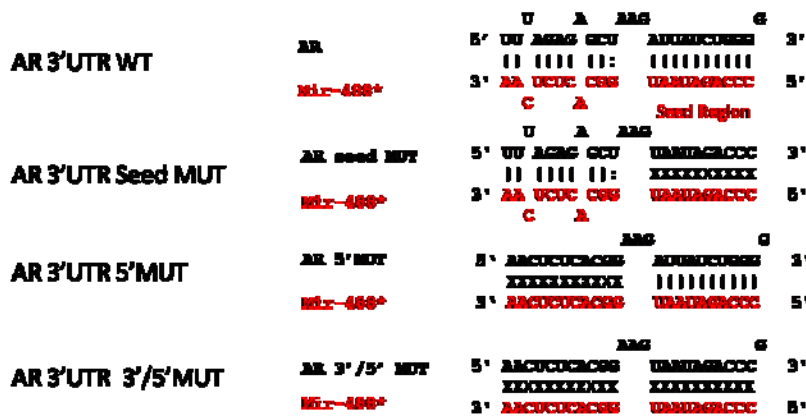


Figure 15: Base pairing interaction between miR-488* and predicted target site: Three constructs were generated, first one harboring mutated seed region, second with mutated bulge region and third with mutated seed region as well as mutated bulge region.

488* is directly interacting with the predicted target site, a new construct harboring the AR 3'UTR with mutated seed region (first 10 nucleotides from 3'

end of the predicted target site) to its complementary

nucleotides was generated as described in "Materials and Method" chapter II. Furthermore, a construct with the 5' half of the predicted target site (bulge region) was mutated to its complementary nucleotides. In addition, another construct harboring both of the previously mentioned mutations within the same target (Figure 15) was designed and generated. The first construct with seed mutations

was named AR 3'UTR seed MUT; the second construct with bulge mutations was named AR 3'UTR 5' MUT and the final construct harboring seed mutations as well as bulge mutations was named AR 3'UTR 3'/5' MUT.

The three mutations were transiently co-transfected into CHO cells with miR-488* mimic and NC mimic as well as renilla luciferase construct as a transfection control with all the appropriate controls. Results are shown in (Figure 16). When cells were transfected with the wild type AR3'UTR chimeric plasmid along with miR-488* mimic, results were similar to previously obtained with repression of luciferase expression of about 55% compared to transfection with NC mimic (Figure 16A).

On the other hand, the co-transfection of the AR 3'UTR seed MUT chimeric plasmid along with miR-488* mimic resulted in down regulation of about 33% compared to NC mimic transfection (Figure 16B). A down regulation of about 58% of luciferase expression was observed when cells were co-transfected with AR 3'UTR 5'MUT along with miR-488* compared to NC mimic (Figure 16C). Unexpectedly, 45 % reduction of luciferase activity was observed when cells were co-transfected with AR 3' UTR 3'/5' MUT with miR-488* mimic compared to NC mimic (Figure 16D).

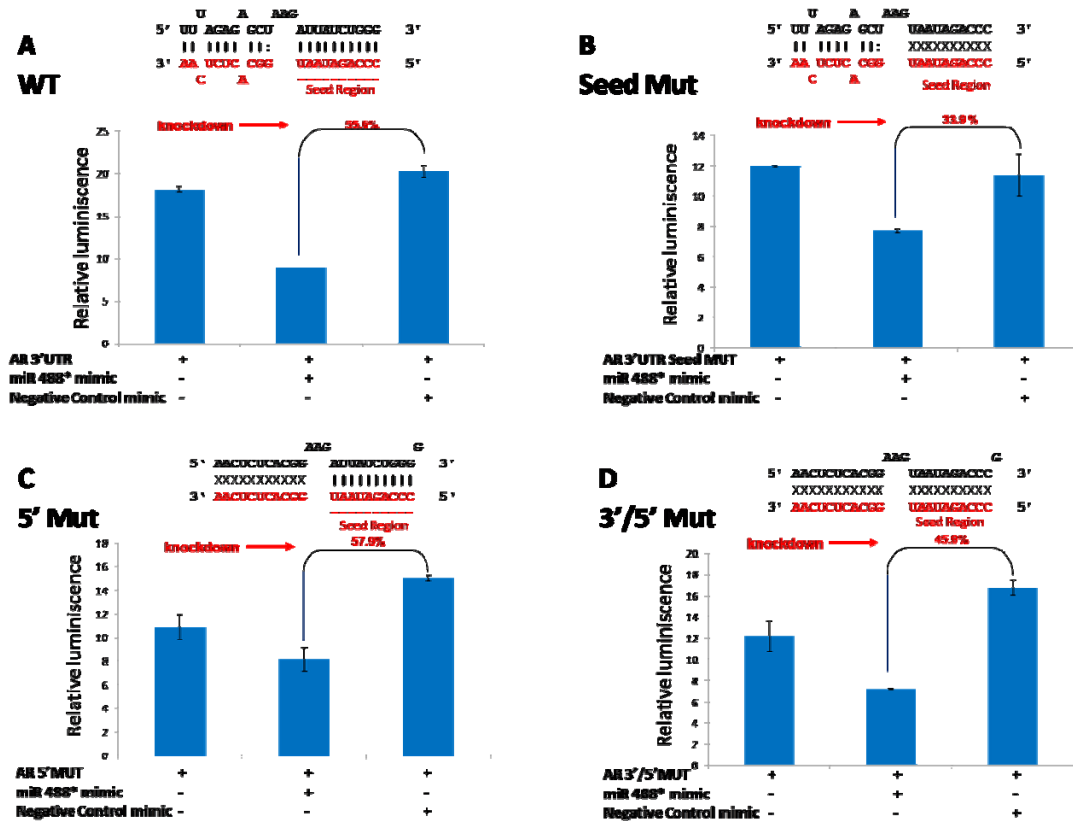


Figure 16: Effect of AR 3'UTR mutations on the levels of luciferase expression in the chimeric plasmid: CHO cells were co-transfected with either wild type AR 3'UTR chimeric plasmid or mutated: **Panel A**, 55% reduction of luciferase expression was observed when transfected with WT AR 3'UTR and miR-488* mimic. **Panel B** 33% reduction of luciferase expression was observed when transfected with AR 3'UTR seed MUT and miR-488* mimic. **Panel C**, 57% reduction of luciferase expression was observed when transfected with AR 3'UTR5' MUT and miR-488* mimic. **Panel D**, 45 % reduction of luciferase expression was observed when transfected with WT AR 3'UTR

Results from panel B and C compared to Panel A, suggest the seed region seems to play a major role in the interaction between the miR-488* and the predicted site in the AR 3'UTR. Nevertheless, results from Panel A and Panel D suggest that there might be other putative sites within the AR 3'UTR mRNA which can interact with miR mimic by Base-pairing. Presumably, these sites are providing miR-488* mimic with substitutionally binding segments, when the first original site (nucleotides 4266-4289) of the AR 3'UTR is mutated. Hence, the down regulation of luciferase expression was still observed even with mutations designed to interrupt interaction between miR-488* and the predicted target site.

3.6 Cloning Shorter AR 3' UTR:

Next question we asked is: Are there any sites that miR-488* is binding to other than the putative site (nucleotides 4266 – 4289)? To address this question, careful observation of the Wild type AR 3'UTR sequence revealed the identity of three sites which might serve as substitution binding sites (Appendix; Fig 4A). Site one (nucleotides 158-168 from 5' end of AR 3'UTR) is consisting of 10 nucleotides with 7 perfect matches to the seed region. Site two (nucleotides 293-299 from 5' end of AR 3'UTR) has 6 nucleotides with 4 perfect matches to the seed region and site three (nucleotides 348-358 from 5' end of AR 3'UTR) is 10 nucleotides with 8 perfect matches to the seed region (Appendix; Fig 4B). Mutation Site Directed Mutagenesis kit (USB Corporation, Cleveland, OH) was used as described in Chapter II, Section 2.4 to individually mutate each newly

revealed sites. Resulted constructs with either mutations in Site I, II or III were co-transfected individually with miR-488* mimic and the appropriate controls. Data showed similar repression levels of fire fly luciferase (54 %, 53% and 52%) for mutated site one, mutated site two and mutated site three, respectively as compared to WT AR 3'UTR with 51% fire fly luciferase repression(Appendix; Fig 5).

These results did not explain neither proves if site one, two and three could serve as substitution binding site for miR-488*. Since we did not have one

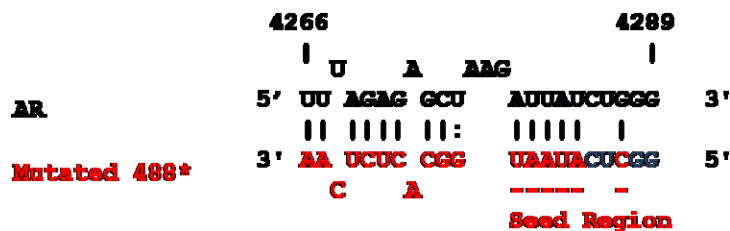


Figure 17: miR-488* mutated mimic alignment with AR 3'UTR: miR-488* mutated mimic; this new negative control have the same nucleotides as miR-488* but with 4 nucleotides to be mutated to its complementary bases in the seed region. Mutated nucleotides are indicated in blue color in seed region.

we decided to clone a shorter segment of AR 3'UTR (nucleotides 561-637 from 5' end of AR 3'UTR (Appendix: Fig 4A & 4B). This segment (77 nucleotides) of AR 3'UTR contained the wild type (Short AR WT) or seed mutated miR-488* target site (Short AR seed MUT) in a luciferase reporter vector. For the following set of experiments a new negative control (miR-488* mut mimic). This new control harboring 4 mutated nucleotides to its complementary bases in the seed region (Figure 17). miR-488* mut mimic was used along with the old negative control from *C. elegans*.

construct harboring all mutated sites as well as the mutated seed region in the putative target site, we decided to clone a shorter segment of AR 3'UTR (nucleotides 561-637 from 5' end of AR

Each of these constructs was co-transfected with either miR-488* mimic or negative control mimic in CHO cells and luciferase activity was measured after 48 hours.

miR-488* reduced luciferase activity of the Short AR WT construct by 30% as compared to that with the NC mimic and miR-488* mut mimic. However, in CHO cells transfected with Short AR seed mut chimeric luciferase reporter plasmid, miR-488* was unable to suppress luciferase activity. Luciferase expression in these cells was similar to that seen in cells co-transfected with Short AR seed mut construct and either NC mimic or miR-488* mut mimic (Figure 18).

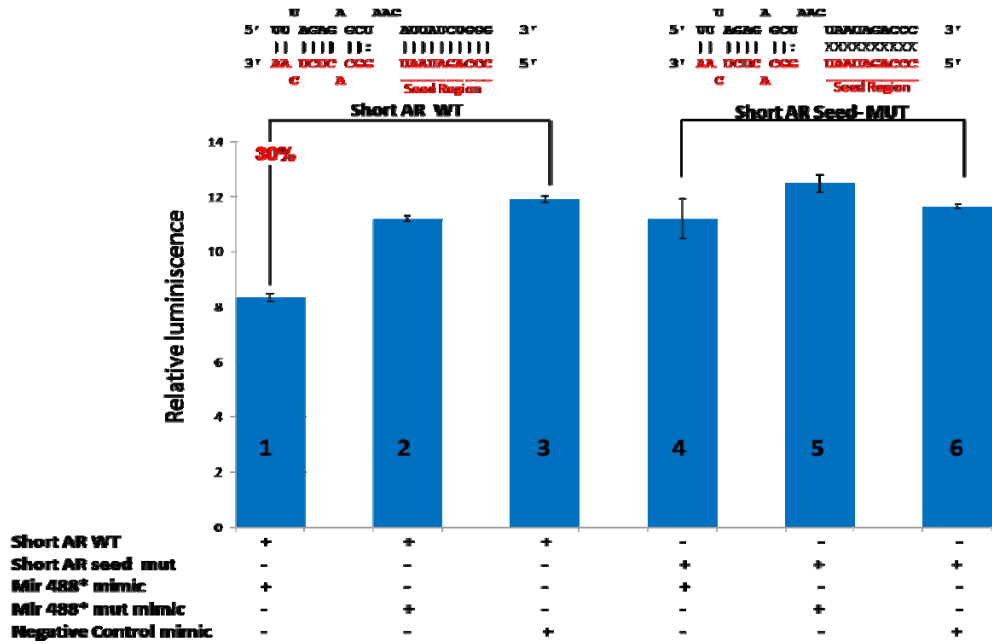
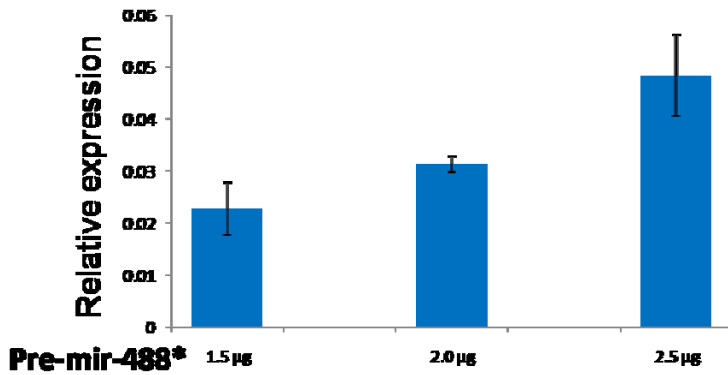


Figure 18: Chimeric plasmid with Shorter AR 3'UTR can be targeted by miR-488*: Mir-488* reduced luciferase activity of the Short AR WT construct by 30% as compared to that with the NC mimic and miR-488* mut mimic. In CHO cells transfected with Short AR seed mut, chimeric luciferase reporter plasmid, miR-488* was unable to suppress luciferase activity. Luciferase expression in these cells was similar to that seen in cells co-transfected with Short AR seed mut construct and either NC mimic or miR-488*

These data suggest that miR-488* putative target site within the shorter AR 3'UTR seems to be an authentic site. Also the reversal of luciferase expression by miR-488* mut mimic suggests that only four nucleotides mutations in the seed region are sufficient enough to disrupt the interaction between miR-488* mimic and predicted target site which is consistent with the common line of thoughts for microRNA mediated gene regulation (Nilsen T, 2007).

3.7 Dose dependent expression of mature miR-488* from Pre-miR-488* expression plasmid:



To study the effects of hsa-miR-488* expressed from its genomic context, an expression reporter system which could

Figure 19: Quantitative Real-Time (qRT) PCR analysis of mature miR-488* expression: An increased dose dependent expression of mature miR-488* was observed respectively to increased concentration of transfected pre-miR-488* chimeric expression vector.

experimentally enable us to express the mature form of miR-488* and

study its effects was required. To achieve this aim, a segment of intron five in ASTN1 gene was PCR amplified from human genomic DNA and cloned between XhoI and BamHI sites of pcDNA 3.1(-) under the expression of CMV promoter. The cloned segment of intron 5 from ASTN 1 gene, codes for hsa-miR-488*

precursor, along with both downstream and upstream flanking regions (Appendix; Fig 6). This construct was named Pre-miR-488*. Overnight grown, 80 % confluent Chinese Hamster Ovary cells were transfected with different concentrations of Pre-miR-488* construct, using polybrene as transfection reagent as described in materials and method. Cells were collected and total RNA was extracted by mean of TRIZOL® Reagent. Quantitative real time PCR technique was used to assess in detecting the mature miR-488* in total RNA aliquots of 10 ng from each transfected concentration samples.

As expected no endogenous expression of miR-488* was detected in untransfected samples. However, samples transfected with increased concentration of pre-miR-488* (1.5, 2.0 and 2.5 µg) showed an increased expression profiles respectively to amount of transfected plasmid expressing genomic miR-488* gene (Figure 19). Cells transfected with 2.5 µg pre-miR-488* expressed mature miR-488* by about 2 fold higher than those transfected with 1.5 µg. These results suggests a dose dependent expression of miR-488* gene in transiently transfected mammalian cells.

3.8 Dose dependent repression of Firefly luciferase expression by Pre-miR-488* :

We have shown that synthetic miR-488* could down regulate the expression of the chimeric luciferase reporter plasmid. Next we investigated whether miR-488* gene can also repress the luciferase activity from the chimeric AR 3'UTR plasmid.

To address this question, we transfected CHO cells with Short AR 3'UTR wild type plasmid and short AR seed MUT plasmid along with increased concentration of the pre-miR-488* expression plasmid. As for controls we transfected a pool of the cells with empty expression plasmid (pcDNA 3.1) and Renilla luciferase plasmid served as internal control for transfection. As shown in Figure 19, Dual luciferase assay's results of samples transfected with increased concentrations of pre-miR-488* (1.5µg, 2.0µg and 2.5µg) have indicated a reduction of luciferase activity of about (10 %, 20 % and 27 %) respectively, to transfected concentration. However the sample of cells transfected with Short AR seed MUT show reversal of luciferase expression similar to results obtained from sample transfected with the empty expression vector. Results were normalized to Renilla expression and represented in (Figure 20).

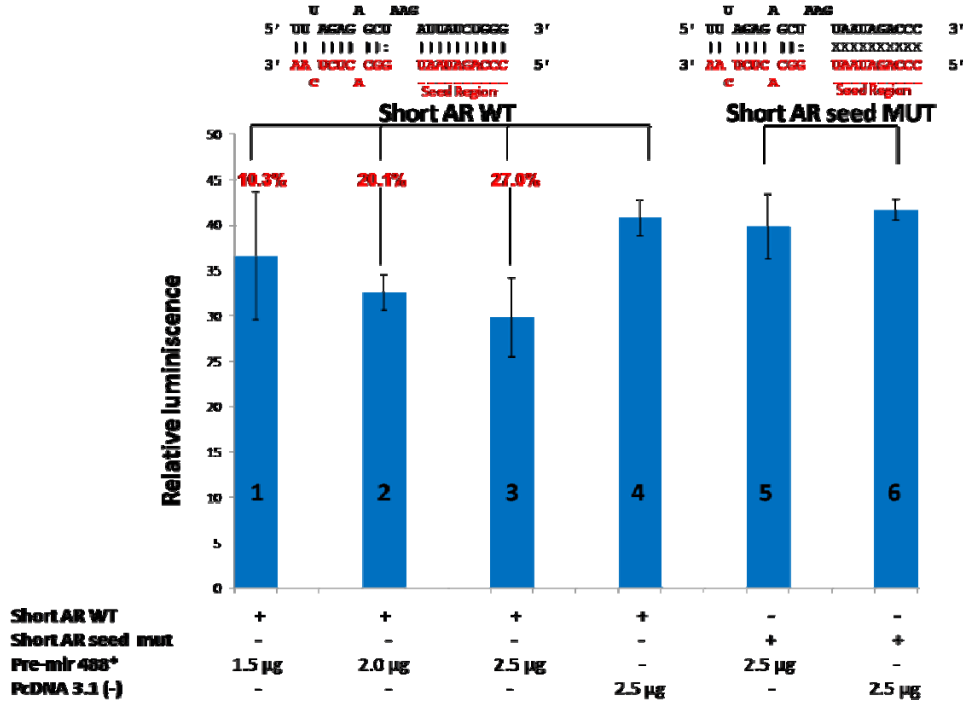


Figure 20: Quantitative analysis of repression of luciferase sensor by Pre-miR-488* expression vector: Luciferase and Renilla expression was measured with increased concentration of transfected pre-miR-488* and with the highest concentration of pcDNA 3.1 empty vector along with the appropriate controls. All expression values and ratio of Firefly to Renilla luciferase were plotted as a measurement of the translational repression of firefly luciferase by ectopically expressed mature miR-488*.

These results were consistent with, observation from induction with synthetic miR-488*. Thus, miR-488* gene expressed from its genomic context have the same ability to target AR 3'UTR and repress the luciferase activity in the chimeric plasmid. miR-488* gene expression profile (Section 3.7) show increased levels of mature miR-488* expression respectively, to increased concentration of transfected pre-miR-488*. Current data (Figure 20) once again enhance the previous observation. The higher the concentration of transfected pre-miR-488*, the higher is the concentration of the expressed mature miR-488*. These results suggest a negative correlation between the amount of transfected pre-miR-488* and the luciferase expression profiles.

3.9 Mutations within miR-488* precursor in different cell lines:

Recent studies indicated that miR-488* predominantly expressed in adrenal gland, adrenal cortex and mainly in brain tissues (Wang E, et al. 2009; Landgraf P et al. 2007). However, we are not aware of any report linking miR-488* to prostate cancer, thus we wanted to explore whether miR-488* is expressed in prostate cells. Unpublished data by our lab have shown that miR-488* is expressed at significantly low levels in androgen dependent cell line (LNCaP) and similar results for the androgen independent cell line (C4-2B). However, no signal for miR-488* was detected from androgen independent cell line DU145.

To further investigate these findings, both Forward and Reverse Pre-488* primers shown in (Table 3; Chapter II) are great tools to perform PCR on genomic DNA collected from several androgen dependent prostate cancer cell line (LNCaP), androgen independent prostate cancer cell lines (DU145, PC3, and CWR 22RV1), Brain tumor cell lines (U-87 and U251) and Human breast adenocarcinoma *cell line* (MDA). Amplified segments were sequenced and analyzed by clustal alignment in (Figure 21), along with the precursor sequence for Hsa-miR-488*.

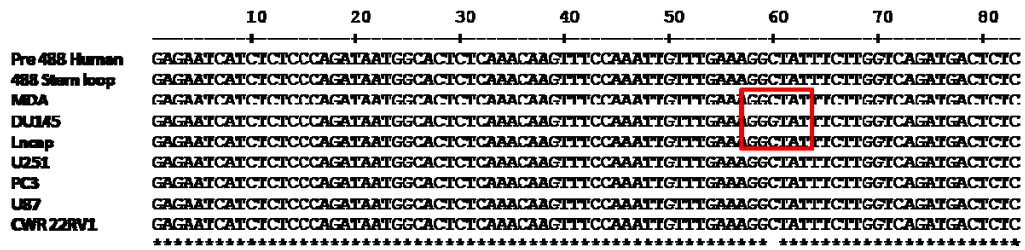


Figure 21: Cluster alignment of miR-488* stem-loop region in different cell lines: sequence alignment of the stem loop region of miR-488* from androgen dependent prostate cancer cell line (LNCaP), androgen independent prostate cancer cell lines (DU145, PC3, and CWR 22RV1), Brain tumor cell lines (U-87 and U251) and Human breast adenocarcinoma cell line (MDA).

Interestingly, all cell lines show high conservation in stem loop region of hsa-

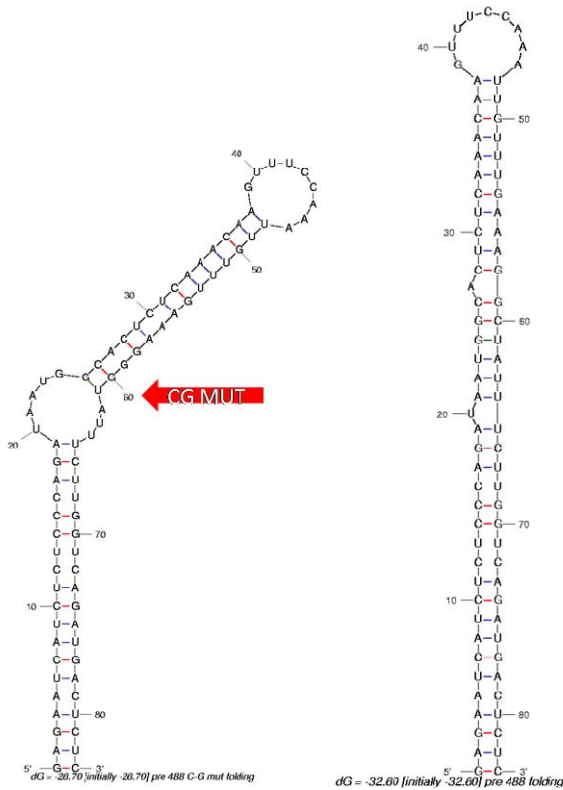


Figure 22: Folding state of miR-488* stem loop: this figure illustrate both folding state of wild type miR-488* stem loop and the corresponded stem loop from DU145 cells (CG mutation at base 60)

miR-488*, with only one point mutation in DU145 cells. This androgen independent cell line incorporated a C to G substitution in nucleotids 60. Interestingly, when both wild type miR-488* stem loop and the corresponded stem loop from DU145 cells (CG mutation at base 60)

folded using RNA-Fold program, it revealed different structure (Figure 22).

It has been proposed that RNA:RNA interactions or RNA:protein interaction are involved in structure recognition and processing precursor miRNA to mature

sequence (Kim *et al* , 2007). These results along with the mature miR-488* expression profile might suggest that the CG mutation at base 60 in DU145 contribute to reduced expression of mature miR-488* in DU145 cell line. Nevertheless, further study is required for better understanding for the role of the CG substitution in the preprocessing of miR-488*.

3.10 Stable cell line (LNCaP and C4-2B) expressing miR-488*:

Androgens stimulate proliferation and inhibit apoptosis, thus maintain the ratio of proliferating cells to those dying. The maintenance of this ratio is very critical for the normal growth of prostate cells (Feldman and Feldman, 2001). In prostate cancer cells this ratio favoring the proliferation. Additionally, AR is required for the proliferation of prostate cells (Feldman & Feldman, 2001; Balk, 2002). However, we have shown in this study that AR is a direct target of miR-488*. Thus, by stably transfecting miR-488* into prostate cancer cells can we once again balance the ratio between proliferation and apoptosis?

To address this question, plasmid DNA Pre-miR-488* was linearized with restriction enzyme, Bgl II and stably transfected into either androgen dependent cell line (LNCaP) or androgen independent cell line (C4-2B). Stably transfected cells were maintained in RPMI 1640 medium supplemented with 10% Fetal bovine serum (FBS), with antibiotics and 100 µg/ml G-148.

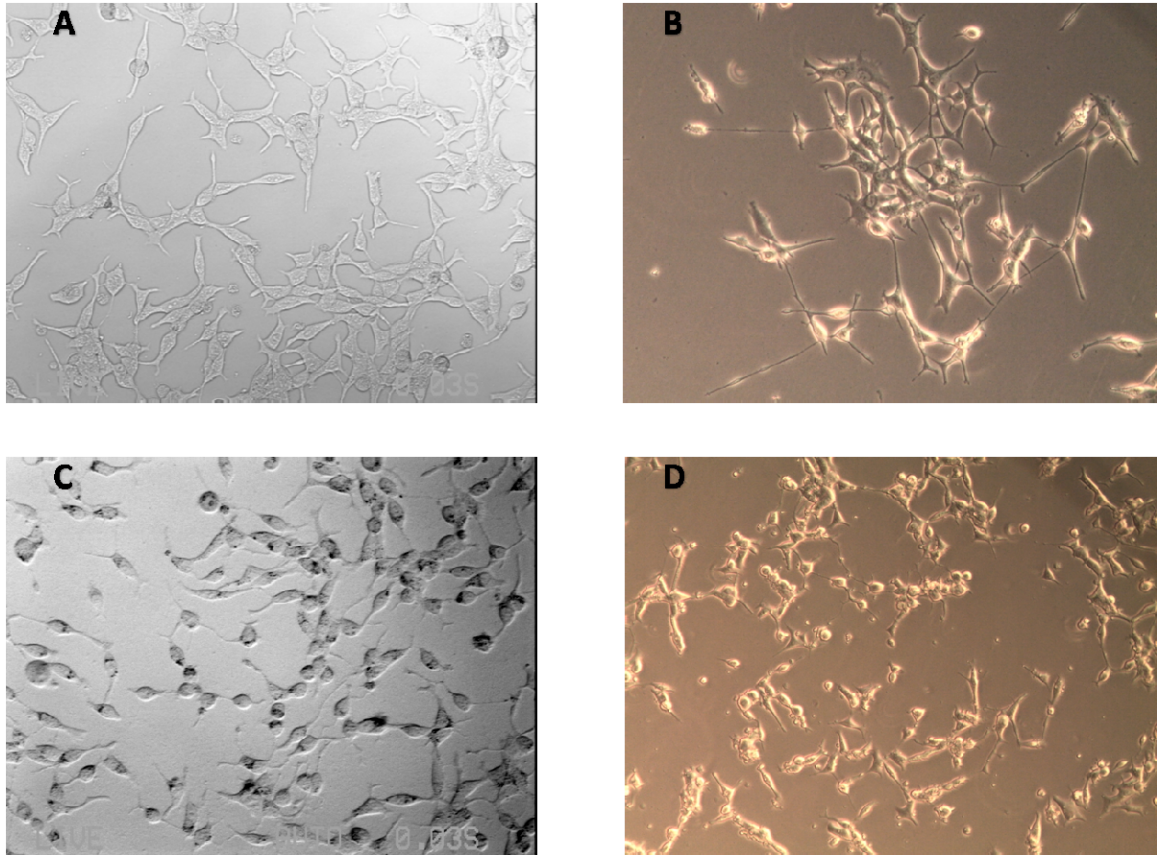


Figure 23: Stable cell line (LNCaP and C4-2B) expressing miR-488*: **Panel A**, Untransfected LNCaP cells, **Panel B**, stably transfected LNCaP cells with Pre-miR-488*. **Panel C**, untransfected C4-2B cells. **Panel D**, stably transfected C4-2B cells with Pre-miR-488*.

This selection media allows for only cells expressing the resisting gene which is incorporated in Pr-miR-488* plasmid to survive. All cell lines were maintained in a humidified 5% CO₂ at 37°C. An interesting observation, that LNCaP cells (androgen dependent) did not grow well and number of cells were low. While C4-2B cells continued to grow and higher number of cells was observed. These results may suggest that more cells are dying to these proliferating in the stably transfect LNCaP cells. On the other hand, it seems that more cells are proliferating to these dying in the C4-2B (androgen independent cell line). We cannot draw a conclusion whether this phenotype is due to the

effect of miR-488* on androgen receptor or not. Further more study is required to enhance our understanding of these two phenotypes.

CHAPTER IV

FUTURE DIRECTIONS AND CONCLUSION

4.1 Implication of the CG substitution in mature miR-488* processing:

It has been proposed that RNA:RNA interactions or RNA:protein interaction are involved in structure recognition and processing precursor miRNA to mature sequence (Kim et al , 2007). MiRNA processing is a compartmentalized process; precursor miRNA at first is made in the nucleus, then it is processed into the mature miRNA in the cytoplasm. In order to study whether the observed CG mutant in DU145 cells is affecting the nuclear process of miRNA precursor or the cytoplasmic process of miRNA maturation; an in vitro system could be used where the precursor sequence for miR-488* is cloned downstream of T7 promoter in one construct. Second construct harboring the precursor sequence for miR-488* along with the observed CG mutation at the indicated position (nucleotide 60) will be cloned downstream of T7 promoter.

After radiolabeling both constructs, they could be used for in vitro miRNA processing system with total cellular extract from DU145 cells or LNCaP cells.

Unpublished data by our lab have shown that miR-488* is expressed at significantly low levels in androgen dependent cell line (LNCaP). However, no signal for miR-488* was detected from androgen independent cell line DU145. These results indicate that the miRNA processing machinery is functional to some degree in LNCaP cells but not in DU145. Thus results from the proposed experiment (see above) with the total cellular extract from LNCaP or DU145 cell lines, could give us some insight whether what is observed from mature miR-488* expression profiles is due to the inactivation of the miRNA processing machinery in DU145 cells or is just simply due to the CG substitution. These experiments may provide an opportunity to identify RNA binding proteins unique to miR-488* stem loop processing.

4.2 Identifying miR-488* precursor promoter:

Hsa-miR-488* is encoded in intron 5 of Astrotactin 1(ASTN1). Intron 5 is a relatively large intron (4.9 kb) gene (Figure 24).

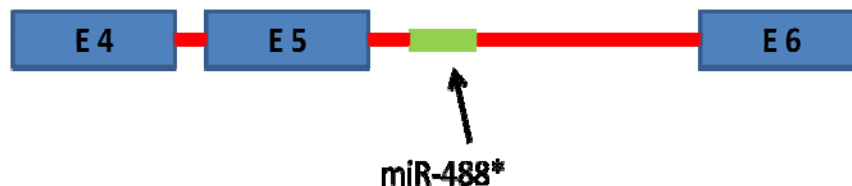


Figure 24: Schematic presentation of the genomic location of miR-488*: MiR-488* is hosted by intron 5 of ASTN 1 gene and preceded by Exon 5, Intron 4 and Exon 4.

Intronic microRNAs studies suggested that microRNAs that reside in introns, share the same promoters and regulatory elements of their host gene

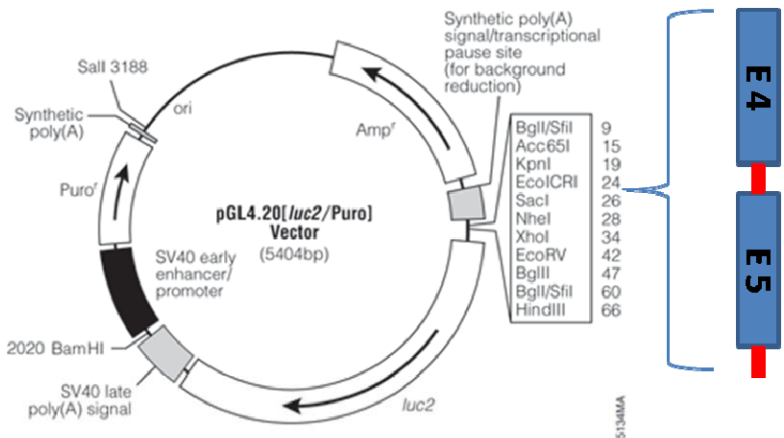


Figure 25: mini gene construct to check for independent promoter activity of miR-488*: including what we think to harbor coding sequence for promoter of miR-488* in ASTN 1 gene. The mini gene construct (Exon 4, intron 4, exon 5 and a segment of intron 5 preceding precursor sequence of miR-488*) is to be cloned into pGL4.20 promoterless luciferase plasmid.

(Sikand *et al.*, 2009). Nevertheless, other miRNA genes are believed to be transcribed from their own promoters. Few primary transcripts have been entirely identified (Lagos-

Quintana *et al.*, 2001; Bartel D P., 2001). Thus to truly understand whether miR-488* has its own promoter or shares the same promoter of its host gene, we could clone the mini gene system harboring Exon4, intron 4, Exon 5 and the segment of intron 5 up to the start of the precursor sequence of miR-488* in the promoterless pGL 4.20 luciferase vector plasmid (Figure 25). Consequently, after transfection of the resulted plasmid into one of the cell lines which previously has shown some levels of endogenous mature miR-488* profiles, we could assay for luciferase activity. The detection of a luciferase activity could mean that the mini gene system is harboring a promoter region. Then, we could identify that specific promoter sequence together along any transcription factors docking sites nearby.

The promoter sequence, if present, could be identified through truncation process of the promoter region. Transcription factor's docking sites, also if present, could be first identified by prediction software's followed by experimental

importance of miR-488* in regulating biological processes. One of the future aims is to build a genome wide library of miR-488* target sites in 3'UTR that allows us to further study the implication of miR-488*.

4.4 Conclusion:

A number of studies have provided insight into molecular mechanisms that contribute to the onset and progression of prostate cancer. Androgens play an important role in the development, regulation, and maintenance of the male phenotype as well as the reproductive physiology and have been implicated in the development and progression of prostate cancer. Androgens are required mitogens for the survival and proliferation of prostate cells and most prostate cancers are treated by complete blockade of androgen. AR is heterogeneously expressed in primary tumors, and throughout the progression of hormone-sensitive and hormone-refractory prostate cancers. AR is a prominent target for the treatment of non-organ confined prostate cancer by hormonal blockade therapy that uses anti-androgens to competitively inhibit the binding of androgen to the ligand binding domain of the receptor. In prostate carcinogenesis, changes in AR signaling pathways activate the growth of malignant cells. The hormone-refractory stage of the disease is commonly associated with the constitutive activation of AR expression by unknown mechanisms.

Noncoding RNAs play diverse functions including structural, enzymatic and regulatory in metazoan gene expression. Genes that are potentially targeted by these miRNAs include cell growth and maintenance, signal transduction, cell proliferation, phosphorylation, cell cycle, transcription factors, cell organization and biogenesis etc. MiRNA mediates gene expression through translational repression of its target by binding at the 3' untranslated region. In this work, our computational analysis has identified a target site of Hsa-miR-488* in the

androgen receptor 3' untranslated region. The chimeric AR3'UTR luciferase plasmid sensor experiment suggested that the predicted target site is an authentic target site. Seed region within target is essential for the binding with miR-488*. Four base pairs mutations to the seed region is enough to disrupt the base pairing interaction between that target site and the miR-488*. Furthermore, western blot data shows repression in the expression of endogenous Human androgen receptor in LNCaP cells by miR-488* mimic. Ectopically expressed mature miR-488* has a dose dependent repression of Firefly luciferase reporter plasmid. Stably expressed miR-488* in androgen dependent prostate cancer cell line (LNCaP) showed slower growth comparing to the miR-488* stably transfected androgen independent cell line (C4-2B).

In conclusion, miR-488* is down regulated in numerous prostate cancer cell lines, suggesting a tumor-inhibitory function of Hsa-miR-488*. That being said, further investigations are required to fully understand the molecular mechanisms underlying the regulation of AR expression by miR-488*. Thus further knowledge of the functions and the mechanisms of miR-488* expression could significantly improve our understanding regarding the use of microRNAs as a therapeutic interventions of prostate cancer.

LITERATURE CITED

1. American Cancer Society. *Cancer Facts & Figures 2009*. Atlanta: American Cancer Society; 2009.. No. 500809
2. Bartel D.P. *MicroRNAs: genomics, biogenesis, mechanism, and function*. Cell. 2004 Jan 23; 116(2):281-97.
3. Bonci D *et al*. *The miR-15a-miR-16-1 cluster controls prostate cancer by targeting multiple oncogenic activities*. Nat Med. 2008 Nov; 14(11):1271-7.
4. Brinkmann AO, *et al*. (1989). *Structure and function of the androgen receptor*. Urol. Res. 17 (2): 87–93.
5. C. Gwizdek, E. Bertrand, C. Dargemont, J.-C. Lefebvre, J.-M. Blanchard, R.H. Singer and A. Doglio, *Terminal minihelix, a novel RNA motif that directs polymerase III transcripts to the cell cytoplasm*, J. Biol. Chem 276 (2001), pp. 25910–25918.
6. Cai X., Hagedorn CH, Cullen BR. *Human microRNAs are processed from capped, polyadenylated transcripts that can also function as mRNAs*. RNA 10, 1957–1966 (2004).
7. Calabro, F., and Sternberg, C. N. (2007). *Current indications for chemotherapy in prostate cancer patients*. Eur Urol 2007; 51:17-26.
8. Calin GA, Sevignani C, Dumitru CD, Hyslop T, Noch E, Yendamuri S, Shimizu M, Rattan S, Bullrich F, Negrini M, Croce C.M. *Human microRNA genes are frequently located at fragile sites and genomic regions involved in cancers*. Proc Natl Acad Sci U S A. 2004 Mar 2;101(9): 2999-3004
9. Campbell N A., Brad W., Robin J.H (2006). *Biology: Exploring Life*. Boston, Massachusetts: Pearson Prentice Hall. ISBN 0-13-250882-6.
10. Chen C.Z *et al*. *MicroRNAs modulate hematopoietic lineage differentiation*. Science. 2004 Jan 2; 303(5654):83-6.
11. Chial, H. (2008) *Tumor suppressor (TS) genes and the two-hit hypothesis*. Nature Education 1(1).
12. Cimmino A, Calin GA *et al*. *miR-15 and miR-16 induce apoptosis by targeting BCL2*. Proc Natl Acad Sci U S A. 2005 Sep 27; 102(39):13944-9.

13. Cooperberg MR, Broering JM, Litwin MS, et al. The contemporary management of prostate cancer in the United States: Lessons from the Cancer of the Prostate Urologic Strategic Research Endeavour (CaPSURE), a National Disease Registry. *J Urol.* 2004; 171:1393–1401.
14. Cotran R. Vinay Kumar, Tucker Collins (1999). *Robbins Pathologic Basis of Disease, 6th Edition.* W.B. Saunders. ISBN 072167335X.
15. Couch DB. *Carcinogenesis: basic principles.* Drug Chem Toxicol. 1996 Aug; 19(3): 133-48.
16. Craft, N., and Sawyers, C. L. *Mechanistic concepts in androgen-dependence of prostate cancer.* Cancer Metastasis Rev 1998-1999; 17:421-427.
17. Culig, Z. et al. *Switch from antagonist to agonist of the androgen receptor bicalutamide is associated with prostate tumor progression in a new model system.* Br J Cancer 1999; 81:242-251.
18. Erdmann, V.A., Szymanski, M., Hochberg, A., Groot, N., and Barciszewski, J. 2000. *Non-coding, mRNA-like RNAs database Y2K.* Nucleic Acids Res. 28: 197-200.
19. Esquela-Kerscher A. and Slack F.J. *Oncomirs - microRNAs with a role in cancer.* Nature Reviews Cancer 6, 259-269 (April 2006).
20. Feldman B.J. and Feldman D. *The development of androgen-independent prostate cancer.* Nature reviews Cancer 2001.
21. Folini M, Gandellini P et al. *miR-21: an oncomir on strike in prostate cancer.* Mol Cancer 9(1):12, 2010.
22. G R Fink, L Adams, J D Watson, J A Innes, B Wuyam, I Kobayashi, D R Corfield, K Murphy, T Jones, R S Frackowiak. *Hyperpnoea during and immediately after exercise in man: evidence of motor cortical involvement.*
23. G R Fink, L Adams, J D Watson, J A Innes, B Wuyam, I Kobayashi, D R Corfield, K Murphy, T Jones, R S Frackowiak. *Hyperpnoea during and immediately after exercise in man: evidence of motor cortical involvement* J Physiol. 1995 December 15; 489(Pt 3): 663–675.
24. Gregory R.I., Yan KP, Amuthan G, Chendrimada T, Doratotaj B, Cooch N, Shiekhattar R. *The Microprocessor complex mediates the genesis of microRNAs.* Nature. 2004 Nov 11; 432(7014):235-40. Epub 2004 Nov 7.

25. György Hutvagner and Phillip D. Zamore. *A microRNA in a Multiple Turnover RNAi Enzyme Complex*. Science 20 September 2002:
26. Harris W., Elahe A Mostaghel, Peter S Nelson and Bruce Montgomery. *Androgen deprivation therapy: progress in understanding mechanisms of resistance and optimizing androgen depletion*. Nat Clin Pract Urol. 2009 Feb; 6(2):76-85.
27. He L. and Hannon G.J. *MicroRNAs: Small RNAs with a Big Role in Gene Regulation*. Nat Rev Genet. 2004 Jul; 5(7):522-31.
28. Imamoto T. *et al. The role of testosterone in the pathogenesis of prostate cancer*. Int J Urol. 2008 Jun; 15(6):472-80. Epub 2008 Apr 22. Review.
29. Jemal A *et al.* (2008) Cancer statistics, 2008. *CA Cancer J Clin* 58: 71–96.
30. Jemal A, Murray T, Ward E, *et al.* *Cancer statistic*. CA Cancer J Clin 2005; 55(1):10-30.
31. Kim V. N. *MicroRNA biogenesis: coordinated cropping and dicing*. Nat Rev Mol Cell Biol. 2005 May;6(5):376-85.
32. Kinzler, Kenneth W.; Vogelstein, Bert (2002). "Introduction". The genetic basis of human cancer (2nd, illustrated, revised ed.). New York: McGraw-Hill, Medical Pub. Division. p. 5. ISBN 978-0-07-137050-9.
33. Kolb FA, Zhang H, Jaronczyk K, Tahbaz N, Hobman TC, Filipowicz W. *Human dicer: purification, properties, and interaction with PAZ PIWI domain proteins*. Methods Enzymol. 2005; 392:316-36.
34. Labrie FMD (2004) Adrenal androgens and intracrinology. *Semin Reprod Med* 22: 299–309.
35. Lagos-Quintana M, Rauhut R, Meyer J, Borkhardt A, Tuschl T. *New microRNAs from mouse and human*. RNA. 2003 Feb; 9(2):175-9.
36. Lagos-Quintana M., Rauhut R., Lendeckel W, Tuschl T. *Identification of novel genes coding for small expressed RNAs*. Science. 2001 Oct 26; 294(5543):853-8.
37. Landgraf P, Rusu M *et al.* *A mammalian microRNA expression atlas based on small RNA library sequencing*. Cell. 2007 Jun 29; 129(7):1401-14.

38. Lau N.C., Lim L.P., Weinstein E.G., Bartel D.P. *An abundant class of tiny RNAs with probable regulatory roles in Caenorhabditis elegans*. *Science*. 2001 Oct 26; 294(5543): 858-62.
39. Lee R.C., Feinbaum R.L., Ambros V. *The C. elegans heterochronic gene lin-4 encodes small RNAs with antisense complementarity to lin-14*. *Cell*. 1993 Dec 3; 75(5):843-54.
40. Lee Y, Ahn C et al. *The nuclear RNase III Drosha initiates microRNA processing*. *Nature*. 2003 Sep 25; 425(6956):415-9.
41. Lee Y, Jeon K et al. *MicroRNA maturation: stepwise processing and subcellular localization*. *EMBO J*. 21, 4663–4670 (2002).
42. Lee YS, Kim HK, et al. *Depletion of Human Micro-RNA miR-125b reveals that it is critical for the proliferation of differentiated cells but not for the down-regulation of putative targets during differentiation*. *J Biol Chem*. 2005 Apr 29; 280(17):16635-41
43. Lee, Y. et al. *MicroRNA genes are transcribed by RNA polymerase II*. *The EMBO Journal* (2004) 23, 4051 – 4060.
44. M.T. Bohnsack, K. Czaplinski and D. Görlich, *Exportin 5 is a RanGTP-dependent dsRNA-binding protein that mediates nuclear export of pre-miRNAs*, *RNA* 10 (2004), pp. 185–191.
45. Marques, R.B. et al. *Androgen receptor modifications in prostate cancer cells upon long-term androgen ablation and antiandrogen treatment*. *Int J Cancer* 2005; 117:221-229.
46. Narry K. and Jin-Wu N. *Genomics of microRNA*. *TRENDS in Genetics* Vol.22 No.3 March 2006.
47. Nazareth L. et al. *Activation of the Human Androgen Receptor through a Protein Kinase A Signaling Pathway*. *Journal of Biological Biochemistry*. Vol. 271, No. 33, Issue of August 16, pp. 19900–19907, 1996.
48. Nilsen T. *Mechanisms of microRNA-mediated gene regulation in animal cells*. *Trends in Genetics* Vol.23 No.5. ScienceDirect 2007.
49. Norman J. Maitland, Anne T. Collins. *Prostate Cancer Stem Cells: A New Target for Therapy*. *Journal of Clinical Oncology*, Vol 26, No 17 (June 10), 2008: pp. 2862-2870Bookmark

50. Parker S.L., Tong T., Bolden S., Wingo PA. Cancer statistics, 1997. CA 1997 ; 47:5-27.
51. Pasquinelli A.E., Reinhart B.J. et al. *Conservation of the sequence and temporal expression of let-7 heterochronic regulatory RNA*. Nature. 2000 Nov 2; 408(6808):86-9.
52. Quigley C.A., De Bellis A. et al. *Androgen receptor defects: historical, clinical, and molecular perspectives*. Endocr Rev 1995 Aug; 16(4):546.
53. R. Yi, Y. Qin, I.G. Macara and B.R. Cullen, *Exportin-5 mediates the nuclear export of pre-microRNAs and short hairpin RNAs*, Genes Dev 17 (2003), pp. 3011–3016.
54. Sawyer SA, Parsch J, Zhang Z, Hartl DL. *Prevalence of positive selection among nearly neutral amino acid replacements in Drosophila*. Proc Natl Acad Sci U S A. (2007) Apr 17; 104(16): 6504-10.
55. Sikand K, Slane SD, Shukla GC. *Intrinsic expression of host genes and intronic miRNAs in prostate carcinoma cells*. Cancer Cell Int. 2009 Aug 12; 9:21.
56. Sinden RR: *DNA Structure and Function*. San Diego: Academic Press; 1994.
57. Sontheimer EJ. *Assembly and function of RNA silencing complexes*. Nat Rev Mol Cell Biol. 2005 Feb; 6(2):127-38.
58. Steven P. Balk. *Androgen receptor as a target in androgen independent prostate cancer*. Urology 60 (suppl 3A): 132-139, 2002.
59. Taneja, S.S. *A multidisciplinary approach to the management of hormone-refractory prostate cancer*, Rev Urol 2003; 2:S53-59.
60. Taplin, M.E., et al. *Selection for androgen receptor mutations in prostate cancers treated with androgen antagonist*. Cancer Res 1999; 59:2511-2515.
61. Varambally, S. et al. *Genomic loss of microRNA-101 leads to overexpression of histone methyltransferase EZH2 in cancer*. Science. 2008 Dec 12; 322(5908):1695-9. Vol.297. no. 5589, pp. 2056 – 2060.
62. Wang D, Lu M, Miao J, Li T, Wang E, et al. *Cepred: Predicting the Co-Expression Patterns of the Human Intronic microRNAs with Their Host Genes*. PLoS ONE. 2009; 4(2): e4421.

63. Wenyong Z., et al. *MicroRNAs in Tumorigenesis*. American Journal of Pathology. 2007; 171:728-738.
64. Wigard P. Kloosterman, Erno Wienholds et al. *Substrate requirements for let-7 function in the developing zebrafish embryo*. Nucleic Acids Res. 2004; 32(21): 6284–6291.
65. Wightman B, Bürglin TR, et al. *Negative regulatory sequences in the lin-14 3'-untranslated region are necessary to generate a temporal switch during Caenorhabditis elegans development*. Genes Dev. 1991 Oct; 5(10):1813-24.
66. Wyngaarden, J.B. & Smith, L.H. Jr (Eds.). (1982). Cecil's Textbook of Medicine: Epidemiology of cancer. Philadelphia, PA: W.B. Saunders Company.
67. Xu-Bao S., Clifford G. et al. *microRNAs and prostate cancer*. J.Cell. Mol. Med. Vol 12, No 5A, 2008 pp. 1456-1465.
68. Yukihide T. and Zamore D. *Perspective: machines for RNAi*. Genes & Dev. 2005. 19: 517-529

APPENDICES

Appendices

miRNAs	Human		Mouse		Rat	
	Gene	Chromosome	Gene	Chromosome	Gene	Chromosome
Mir-26b	Ctdsp1	2	Ctdsp1	1	Ctdsp1	9
Mir-28	Lpp	3	Lpp	16	Lpp	11
Mir-103-1	Pank3	5	Pank3	11	Pank3	10
Mir-103-2	Pank2	20	Pank2	2	Pank2	3
Mir-107	Pank1	10	Pank1	19	Pank1	1
Mir-204	Trpm3	9	Trpm3	19	Trpm3	1
Mir-211	Trpm1	15	Trpm1	7	Trpm1	1
Mir-326	Arb1	11	Arb1	7	Arb1	1
Mir-330	Eml2	19	Eml2	7	Eml2	1
Mir-361	Chm	X	Chm	X	Chm	X
Mir-378	Ppargc1b	5	Ppargc1b	18	Ppargc1b	18
Mir-455	Col271a	9	Col271a	4	Col271a	5
Mir-483	Igf2	11	Igf2	7	Igf2	1
Mir-488*	Astn1	1	Astn1	1	Pseudogene	13
Mir-499	Myh7b	20	Myh7b	2	Myh7b	3
Mir-652	Tmem164	X	Tmem164	X	Tmem164	X

Table 1: Host genes, chromosomes and miRNA distribution: The table illustrates examples of conserved miRNAs with their host genes and gene IDs.

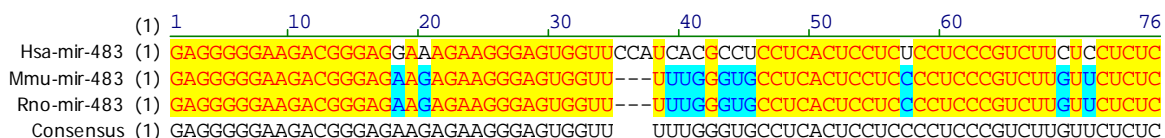


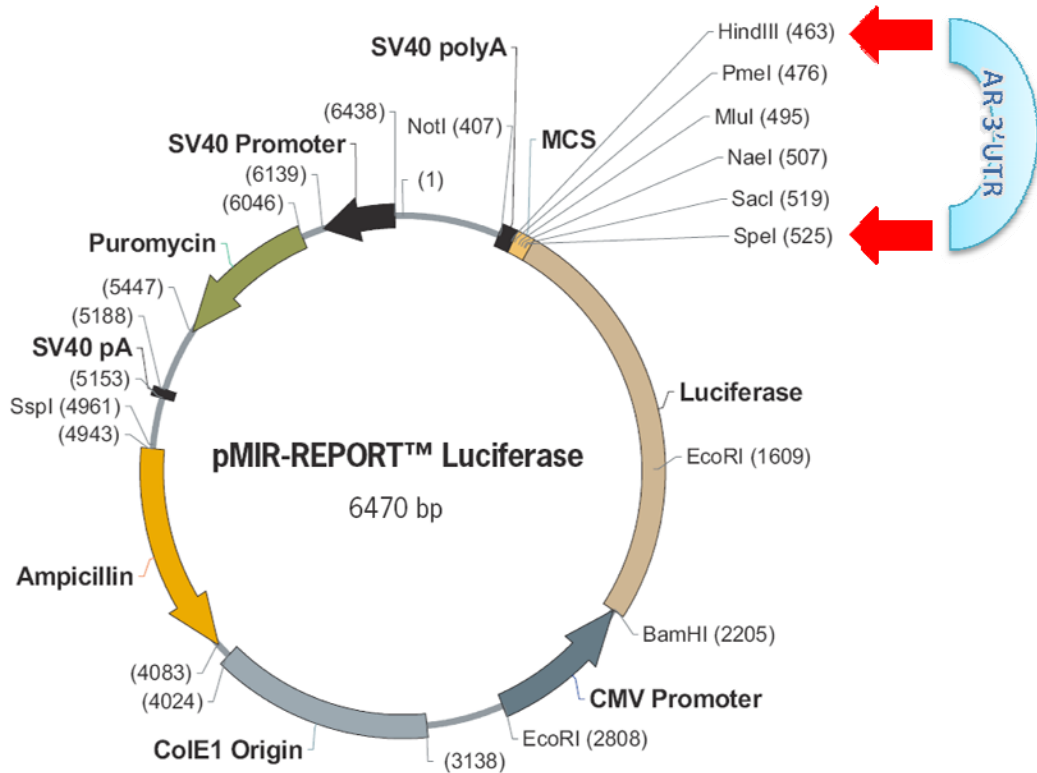
Figure 1: Alignments of the stem loop of miRNAs 483 of human, mouse and rat : The figure illustrates a representative dataset showing conserved sequence elements found in stem loop sequences of the miRNA of human, mouse and rat. An 81.5% of total conservation is observed.

```

1      CCTCCTTGTC AACCCCTGTTT TTCTCCCTCT TATTGTTCCC TACAGATTGC GAGAGAGCTG
61     CATCAGTTCA CTTTTGACCT GCTAATCAAG TCACACATGG TGAGCGTGGA CTTTCCGGAA
121    ATGATGGCAG AGATCATCTC TGTGCAAGTG CCCAAGATCC TTTCTGGGAA AGTCAAGCCC
181    ATCTATTTCC ACACCCAGTG AAGCATTGGA AACCCATTTT CCCCACCCCA GCTCATGCCC
241    CCTTTCAGAT GTCTTCTGCC TGTTATAACT CTGCACTACT CCTCTGCAGT GCCTTGGGGA
301    ATTTCTCTA  TTGATGTACA GTCTGTCATG AACATGTTCC TGAATTCTAT TTGCTGGGCT
361    TTTTTTTTTCT CTTTCTCTCC TTTCTTTTTTC TTCTTCCCTC CCTATCTAAC CCTCCCATGG
421    CACCTTCAGA CTTTGCTTCC CATTGTGGCT CCTATCTGTG TTTTGAATGG TGTGTATGC
481    CTTTAAATCT GTGATGATCC TCATATGGCC CAGTGTCAAG TTGTGCTTGT TTACAGCACT
541    ACTCTGTGCC AGCCACACAA ACGTTTACTT ATCTTATGCC ACGGGAAGTT TAGAGAGCTA
601    AGTAATAGAC CCGAAATCAA AACAAAAACA AGCAAAC

```

Figure2: Androgen Receptor 3' untranslated region. The figure illustrates the AR 3'UTR sequence (637 bases) with the predicted target site of miR-488* underlined and highlighted in red color. Target site consists of 24 nucleotides between base 589 and base 612.



Assay for mRNA specific miR Function

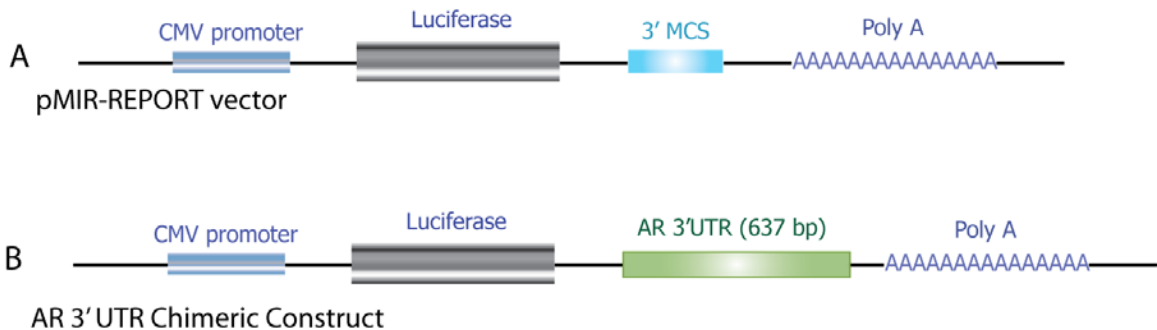


Figure 3: pMIR-Report and an assay for mRNA specific miR function. The figure represents pMIR-Report Luciferase vector with the two restriction sites (SpeI and HindII) at the far ends of the MCS. Figure 3A and 3B are an illustration of the assay for AR

3'UTR specific microRNA function. Figure 3A is a representation of luciferase gene cloned downstream of CMV promoter. Figure 3B is the chimeric luciferase sensor plasmid with AR3'UTR downstream of the luciferase gene.

A

```

1 CCTCCTTGTC AACCCCTGTTT TTCTCCCTCT TATTGTTCCC TACAGATTGC GAGAGAGCTG
61 CATCAGTTCA CTTTGGACCT GCTAATCAAG TCACACATGG TGAGCGTGGG CTTTCCGGAA
121 ATGATGGCAG AGATCATCTC TGTGCAAGTG CCCAAGATCC TTTCTGGGAA AGTCAAGCCC Site 1
181 ATCTATTTCC ACACCCAGTG AAGCATTGGA AACCTTATTT CCCACGCCA GCTCATGCCC
241 CCTTTCAGAT GTCTTCTGCC TGTATAACT CTGCACTACT CCTCTGCAGT GCCTTGGGGA Site 2
301 ATTTCCCTCTA TTGATGIACA GTCTGTCAAT AACATGTTCC TGAATTCTAT TTGCTGGGCT Site 3
361 TTTTTTTTCT CTTTCTCTCC TTTCTTTTTC TTCTTCCCTC CCTATCTAAC CCTCCCATGG
421 CACCTTCAGA CTTTGCCTCC CATTGTGGCT CCTATCTGTG TTTTGAATGG TGTGTATATGC
481 CTTTAAATCT GTGATGATCC TCATATGGCC CAGTGTCAAG TTGTGCTTGT TTACAGCACT
541 ACTCTGTGCC AGCCACACAA ACGTTTACTT ATCTTATGCC ACGGGAAGTT TAGAGACCTA
601 AGATTATCTG GGGAAATCAA AACAAAAACA AGCAAAC

```

Figure 4A: AR 3' UTR with three substitution binding sites for miR-488*. miR-488* substitution sites are indicated as site 1, site 2 and site 3. Bases are highlighted in red. These three sites might serve as substitution targets for miR-488*.

B

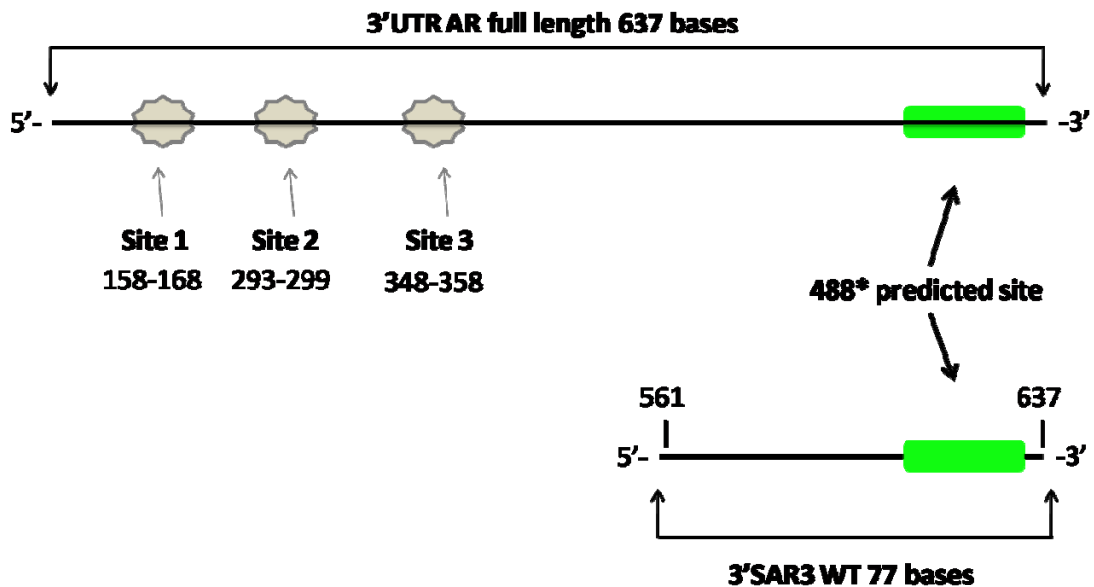


Figure 4B: Schematic representation of segments of AR3'UTR cloned in pMIR report vector. Full length AR3'UTR (637 bases) with the miR-488* predicted site is

shown in green box. Site 1 (nucleotides 158-168 from 5' end of AR 3'UTR) consists of 10 nucleotides with 7 perfect matches to the seed region. Site 2 (nucleotides 293-299 from 5' end of AR 3'UTR) has 6 nucleotides with 4 perfect matches to the seed region and Site 3 (nucleotides 348-358 from 5' end of AR 3'UTR) is composed of 10 nucleotides with 8 perfect matches to the seed region. Short AR 3'UTR (77 bases) spanning between nucleotide 561 and nucleotide 637.

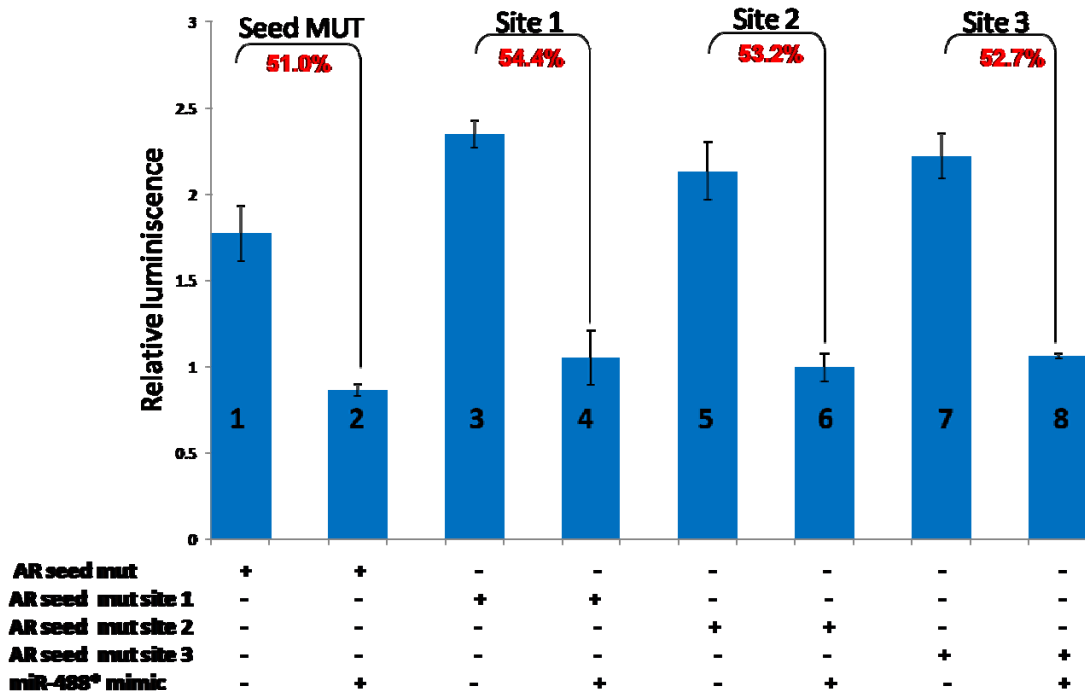


Figure 5: Quantitative analysis of the repression of Luciferase sensor harboring individual mutations to site 1 , site 2 and site 3 by miR-488* mimic. Repression levels of firefly luciferase (54%, 53% and 52%) for mutated site 1, mutated site 2 and mutated site 3 respectively as compared to seed MUT AR 3'UTR with 51% firefly luciferase repression.

1 10 20 30 40 50
 | | | | | |
 GTAAAGGATCTGGGAGTGAGGGAGGCGGGGAAGGCCAAGAGGTGTTGGG
 TTGGGTTGTGGGCTCTATGGAACAAAACCAGTTTCTGCAAGAAGAATTTT
 TGGACCACAACCTGGTGTTCCTCCTAAGGAAGAAAGAAGAGCCTAGAGTG
 GAAAATTTCA**GAGAATCATCTCTCCAGATAATGGCACTCTCAAACAAGT**
TTCCAAATTGTTTGAAAGGCTATTTCTTGGTCAGATGACTCTCAATTTCT
 TCTGGAAGACTCAGGAGTCATATTTTGCTGTTTCAGACAAAACAAAGTTAAT
 AAAGTGTGTTGTATGTGAAAAGATGGATACTATATGTACCCCTGCTTCCT
 CTACCACATTGGCCTTGGGTTTGAGCTAGGCAAGGATTGGGGGCAGTGTA
 GTT

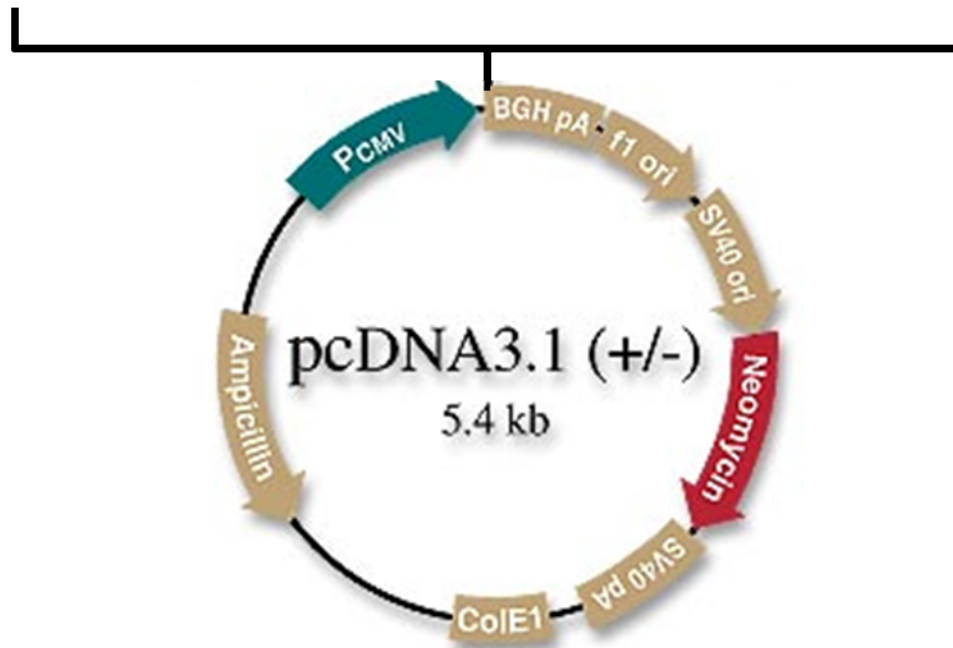


Figure 6: Pre-miR-488* expression vector. The 383bp segment of intron five of ASTN1 containing precursor sequence for miR 488* and flanking region was PCR amplified and cloned downstream of CMV promoter into the MCS of pcDNA 3.1 (-) vector.

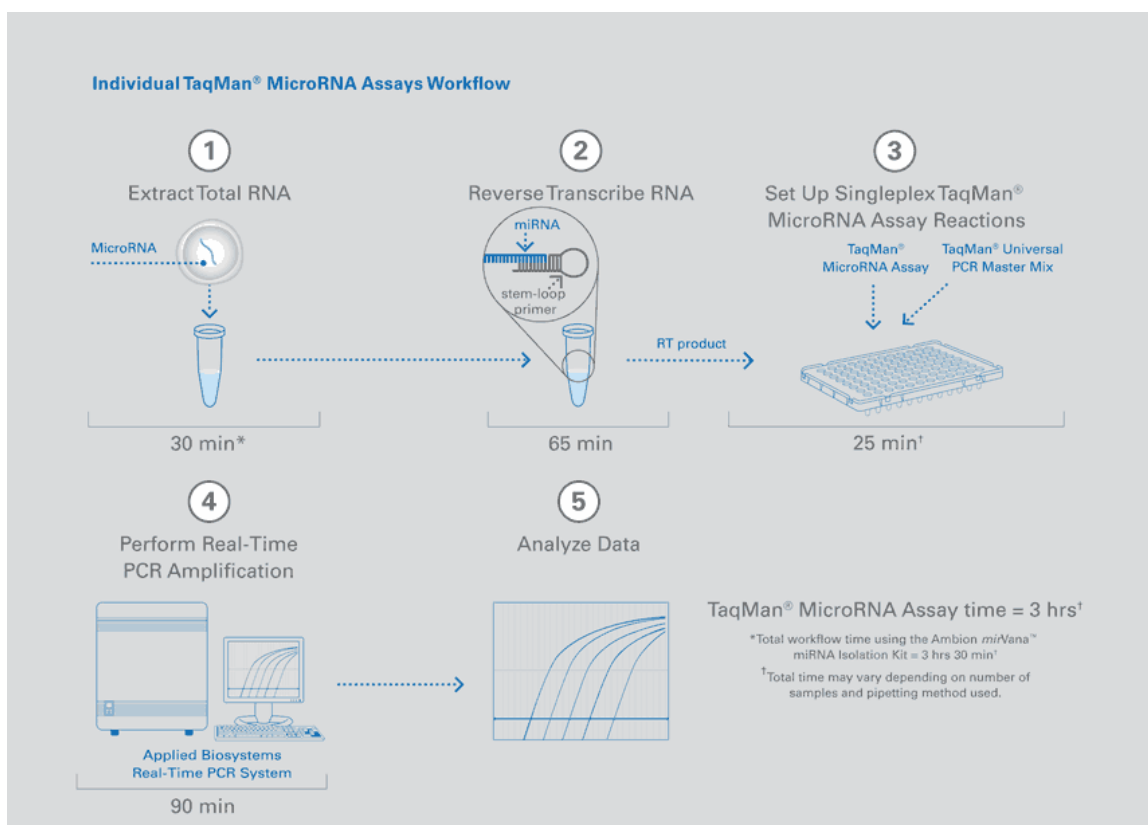


Figure 7: TaqMan MicroRNA Assay. The step one shows the extraction of total RNA. Step 2 illustrates the Reverse Transcription of RNA. The step 3 demonstrates the set up of Singleplex taqMan microRNA Assay reaction. Finally, the step 4 shows the Real-time PCR amplification followed by analysis of the data in step 5.